

***Magnaporthe grisea* Cutinase2 Mediates Appressorium Differentiation and Host Penetration and Is Required for Full Virulence**

Pari Skamnioti and Sarah J. Gurr¹

Department of Plant Sciences, University of Oxford, Oxford OX1 3RB, United Kingdom

The rice blast fungus *Magnaporthe grisea* infects its host by forming a specialized infection structure, the appressorium, on the plant leaf. The enormous turgor pressure generated within the appressorium drives the emerging penetration peg forcefully through the plant cuticle. Hitherto, the involvement of cutinase(s) in this process has remained unproven. We identified a specific *M. grisea* cutinase, *CUT2*, whose expression is dramatically upregulated during appressorium maturation and penetration. The *cut2* mutant has reduced extracellular cutin-degrading and Ser esterase activity, when grown on cutin as the sole carbon source, compared with the wild-type strain. The *cut2* mutant strain is severely less pathogenic than the wild type or complemented *cut2/CUT2* strain on rice (*Oryza sativa*) and barley (*Hordeum vulgare*). It displays reduced conidiation and anomalous germling morphology, forming multiple elongated germ tubes and aberrant appressoria on inductive surfaces. We show that Cut2 mediates the formation of the penetration peg but does not play a role in spore or appressorium adhesion, or in appressorial turgor generation. Morphological and pathogenicity defects in the *cut2* mutant are fully restored with exogenous application of synthetic cutin monomers, cAMP, 3-isobutyl-1-methylxanthine, and diacylglycerol (DAG). We propose that Cut2 is an upstream activator of cAMP/protein kinase A and DAG/protein kinase C signaling pathways that direct appressorium formation and infectious growth in *M. grisea*. Cut2 is therefore required for surface sensing leading to correct germling differentiation, penetration, and full virulence in this model fungus.

INTRODUCTION

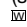
The cuticle covers all aerial plant parts and constitutes the first physical obstacle to pathogen ingress and infection. It comprises a hydrophobic cutin network of interesterified hydroxy and epoxy fatty acid derivatives, overlaid and partially intermingled with wax, and represents a formidable barrier to breach (Lequeu et al., 2003; Nawrath, 2006). Pathogenic fungi effect entry into the host plant by diverse strategies, ranging from entry via natural portals, such as stomata, to direct penetration of the cuticle. To penetrate the cuticle, fungi produce cutinases, extracellular Ser esterases that hydrolyze cutin (Kolattukudy, 1985; Kolattukudy et al., 1995b). Several tangible lines of evidence support a crucial role for cutinase in plant penetration by certain fungi (Maiti and Kolattukudy, 1979; Koller et al., 1991, 1995; Rogers et al., 1994; Kolattukudy et al., 1995a, 1995b). Upon host contact, spores of *Fusarium solani* f. sp. *pisi* release small amounts of constitutively expressed cutinase; the resulting plant-derived C₁₆-C₁₈ cutin monomers act in conjunction with a soluble nuclear protein factor to activate the transcription at high levels of a cutinase gene assisting penetration (Woloshuk and Kolattukudy, 1986; Podila

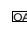
et al., 1988; Li et al., 2002). In fact, heterologous expression of an *F. solani* cutinase gene in the cutinase-deficient, wound-only fungus *Mycosphaerella* spp rendered it capable of infecting papaya (*Carica papaya*) through the intact cuticle (Dickman et al., 1989). Subsequently, however, none of the cutinase knockout mutants generated in a range of phytopathogenic fungi have provided evidence to support a definitive role for cutinase in penetration of the cuticle (Chasan, 1992; Stahl and Schafer, 1992; Stahl et al., 1994; Yao and Koller, 1995; Crowhurst et al., 1997; van Kan et al., 1997; Li et al., 2003; Reis et al., 2005).

Similarly, there is no unequivocal molecular evidence that cutinase facilitates penetration in fungi employing specialized infection cells, called appressoria, to infect living host cells (Sweigard et al., 1992a; Yao and Koller, 1995). Instead, cuticle rupture has been demonstrated to be by the exertion of enormous physical force (Howard et al., 1991; Bechinger et al., 1999). Cutinase was shown to be required for spore adhesion of the rust fungus *Uromyces viciae-fabae* (Deising et al., 1992) and proposed to be involved in adhesion in *Colletotrichum graminicola* (Pascholati et al., 1993) and *Blumeria graminis* f. sp. *hordei* (Pascholati et al., 1992). Cutinase has also been postulated to play a role in carbon acquisition during subcuticular growth of *Venturia inaequalis* (Koller et al., 1991). In addition, cutin monomers are known to promote germ tube and appressorium differentiation on chemically inert surfaces in both *B. graminis* f. sp. *hordei* (Francis et al., 1996; Zhang et al., 2005) and *Magnaporthe grisea* (Gilbert et al., 1996; DeZwaan et al., 1999). Cutin monomers also enhance resistance to infection by *M. grisea* and *B. graminis* f. sp. *hordei* (Schweizer et al., 1994, 1996). Similarly,

¹ Address correspondence to sarah.gurr@plants.ox.ac.uk.

The author responsible for distribution of materials integral to the findings presented in this article in accordance with the policy described in the Instructions for Authors (www.plantcell.org) is: Sarah Gurr (sarah.gurr@plants.ox.ac.uk).

 Online version contains Web-only data.

 Open Access articles can be viewed online without a subscription. www.plantcell.org/cgi/doi/10.1105/tpc.107.051219

plant cutin mutants, displaying plant developmental abnormalities (Sieber et al., 2000; Kurdyukov et al., 2006), showed immunity to attack by the necrotrophic fungus *Botrytis cinerea* (Bessire et al., 2007; Chassot et al., 2007). Therefore, the cuticle appears to be involved in signal exchange between plant and pathogen and important for plant defense and development.

The rice blast fungus *M. grisea* is the most destructive pathogen of cultivated rice (*Oryza sativa*), the staple diet of half of the world's population, while it also infects >50 grass species, including wheat (*Triticum aestivum*) and barley (*Hordeum vulgare*) (Talbot, 2003). *M. grisea* has also emerged as a model biotrophic fungus for the study of plant-microbe interactions (Valent, 1990; Talbot, 2003; Dean et al., 2005; Gilbert et al., 2006). It offers the classical example of mechanically powered entry into the host with sophisticated biochemical and cellular processes underpinning the accumulation of glycerol-generated turgor pressure within the rigid, melanin-pigmented appressorium (Howard et al., 1991; deJong et al., 1997; reviewed in Wang et al., 2005). Turgor can reach 8 MPa, the highest pressure known in any biological system, immediately preceding emergence of a slender hypha, the penetration peg (Howard et al., 1991). This peg effectively ruptures the plant cuticle and cell wall to invade the underlying epidermal cell (Howard and Valent, 1996). Such brute force is crude but effective as the host cell response to invasion is minimal. However, while Howard et al. (1991) defined the magnitude of the turgor pressure powering appressorium peg penetration, they did not discount a role for extracellular enzymes in host penetration. Sweigard et al. (1992a, 1992b) identified a cutin-degrading enzyme, encoded by the *CUTINASE1* (*CUT1*) gene, which was dispensable for pathogenicity, but nonetheless the data inferred that other factors may be involved in enzymatic penetration in *M. grisea*. Indeed, seven more members of a cutinase family were revealed in the *M. grisea* genome (Dean et al., 2005) and, subsequently, 16 putative cutinases in genome sequence release 5. This provided the basis for our attempts to elucidate whether cutinase does in fact assist mechanical penetration in the rice blast fungus.

M. grisea produces a prolific number of infective asexual spores. Upon landing on a host leaf, the three-celled conidium exudes an apical droplet of spore tip mucilage that adheres it to the host (Hamer et al., 1988). Over the next 30 min, a short germ tube emerges from the spore and attaches the germling to the substrate via secreted extracellular matrix (ECM) (Bourett and Howard, 1990). The apex of the germ tube (15 to 30 μ m in length) swells, hooks, presses down onto the plant surface, and initiates appressorium formation. This process of hooking is considered to be pivotal as the germling perceives the substrate characteristics prior to commitment to full appressorium formation (Bourett and Howard, 1990; Howard and Valent, 1996). The correct combination of topographic and chemical signals—surface hardness, hydrophobicity, and absence of exogenous nutrients—trigger signal transduction cascades and the formation of the mature appressorium (Kamamura et al., 2002; Talbot, 2003; Liu et al., 2007).

Downstream of surface contact and chemical sensing, a considerable research effort has unmasked much about the role of the cAMP signal transduction pathway (Lee and Dean, 1993; Xu and Hamer, 1996; Xu et al., 1997; Adachi and Hamer, 1998; Lee

et al., 2003; Dean et al., 2005), G-coupled proteins and their regulators (Liu and Dean, 1997; Nishimura et al., 2003; Liu et al., 2007), and mitogen-activated protein (MAP) kinase cascades (Xu and Hamer, 1996; Choi and Dean, 1997; Xu et al., 1998; Park et al., 2002; Zhao et al., 2005) in the control of appressorium formation and in host penetration by *M. grisea*. Far less is known about signal transduction via protein kinase C (PKC) pathways (Thines et al., 1997b, 1997a; Zhang et al., 2001; Carver and Gurr, 2006). Moreover, there are few documented reports attesting to a proven link between surface perception and signal transduction relay (Liu and Dean, 1997; DeZwaan et al., 1999). Here, we highlight the *M. grisea* transmembrane protein Pth11 as a likely upstream effector of appressorium differentiation in response to surface cues (DeZwaan et al., 1999). However, this story was made more complex by the recent discovery that the *M. grisea* genome carries another 60 G protein-coupled receptor (GPCR)-like proteins related to *PTH11* (Kulkarni et al., 2003, 2005; Dean et al., 2005).

The role of cutinases in fungal penetration has been debated for decades, yet it still remains controversial. Much of the work has focused on cutinases not expressed in parasitic growth (Yao and Koller, 1995) and was in ignorance of the numbers of cutinase genes present within a given fungal genome. We present genetic evidence that the *M. grisea* virulence determinant *CUT2* is crucially involved in the induction of signal transduction pathways leading to true germling morphogenesis and successful plant penetration. We provide direct evidence of the involvement of cutinase in penetration in this model phytopathogen.

RESULTS

Three Putative Cutinase Genes Are Differentially Expressed during Appressorium Formation on Infection-Related Artificial Surfaces

We reanalyzed the genome microarray data of Dean et al. (2005) by angular distribution decomposition (Lees et al., 2007). These data track the changing transcript levels of 13,666 ESTs in *M. grisea* germlings at 0, 7, and 12 h postinoculation (hpi), comparing germling differentiation on two artificial surfaces: a hydrophobic surface inductive to appressorium formation and a hydrophilic noninductive surface. We compared transcript levels in germlings at 7 and 12 hpi with the ungerminated spores (0 hpi). Angular distribution decomposition highlighted the transcript profiles of three particular cutinases. Two of them, MGG11966 (renamed in genome release 5 from merged sequences MGG11108 and MGG02301 recorded in genome annotation 4; Dean et al., 2005) and MGG09100, fall into a cluster of genes with transcript levels greatly upregulated at 12 hpi and moderately upregulated at 7 hpi on the inductive surface but with little change in expression at 12 or 7 hpi on the noninductive surface (Lees et al., 2007). The remaining cutinase EST, MGG2393, falls into another gene cluster, where there is large upregulation in transcript activity at 12 hpi but no regulatory change at 7 hpi on the inductive surface and relatively small downregulation at 12 hpi on the noninductive surface. However, these data are derived from in vitro experiments with infection-related and noninfection-related surfaces. While the inductive surface mimics the leaf and

provides us with an assessment of transcript levels during germling differentiation, the data fall short of assessing *in vivo* penetration-related transcripts. We therefore conducted a detailed analysis of the temporal expression of the three highlighted genes during the ectopic developmental stages, penetration, and *in planta* growth of *M. grisea*.

Three Putative Cutinase Genes Are Differentially Expressed during Penetration *In Vivo*

We used quantitative real-time RT-PCR to fine-profile the changes in transcript activity of MGG09100, MGG11966, and MGG02393 in *M. grisea* rice pathogenic strain Guy11 germlings differentiating on barley leaves. Tissue was analyzed from ungerminated spores harvested from 10-d-old cultures *in vitro* (0 h) and from six time points after spores were inoculated onto the leaves: coincident with spore adhesion and initial host perception (0.5 h), germ tube emergence (1 h), germ tube elongation and initial tip apical swelling (2 h), differentiation of the hooked appressoria (5 h), maturation of the melanized appressoria and penetration (12 h), and *in planta* growth (48 h) (Figure 1). The timing of stage-specific germling development, maturation of appressoria, and subsequent penetration events has been described previously in barley (Skamnioti et al., 2007). As the *M. grisea* cutinases are members of a highly conserved multigene family (see Supplemental Table 1 online), much care was taken to design quantitative real-time RT-PCR primer pairs that amplified nonhomologous and nonoverlapping regions of individual genes and that preferably spanned introns. Moreover, all data were independently normalized against two constitutively expressed genes, β TUB (MGG00604) and *EGF1* (MGG03641) (Skamnioti et al., 2007). Transcript abundance of *M. grisea* MGG02393 *in vivo* revealed the gene to be nominally upregulated during spore attachment (0.5 and 1 h) and approximately threefold more abundant, compared with 1 hpi, during the melanization of appressoria and penetration (12 h) (Figures 1A and 1B). This is at variance with the data derived from *in vitro* experiments recorded in Dean et al. (2005). By contrast, *M. grisea* MGG11966 is negligibly expressed during early germling morphogenesis but upregulated by 50-fold compared with β TUB (70-fold with *EGF1*) during penetration (12 hpi) (Figures 1C and 1D). MGG09100 is significantly upregulated (750-fold compared with β TUB; 500-fold compared with *EGF1*) during germ tube and appressorium differentiation (2 and 5 hpi) and dramatically upregulated (2700-fold compared with β TUB; 4500-fold compared with *EGF1*) at 12 hpi (Figures 1E and 1F). These data agree with the findings of Dean et al. (2005); however, the degree of change at 12 hpi is significantly greater *in vivo* than *in vitro*. The striking expression pattern of MGG09100, particularly coincident with penetration, rendered this gene (designated *CUT2*; *CUT1* was studied by Sweigard et al., 1992a; 1992b) the obvious candidate to knock-out in our quest to unmask whether cutinase is involved in host penetration in *M. grisea*.

Construction of a *cut2* Knockout Mutant and a *cut2/CUT2* Reconstituted Strain

The coding region of *CUT2* is a 495-bp open reading frame interrupted by two short introns. The translated sequence has a

putative secretory peptide of 18 amino acids and carries the hallmark motifs of conserved amino acid sequences surrounding the cutinase catalytic triad of Asp, Ser, His (Martinez et al., 1992). To determine the function of *Cut2*, we performed a targeted gene disruption. We constructed a *CUT2* gene disruption vector, pPS21, by introducing the antibiotic Hygromycin B resistance gene between two *Xho*I sites into the 5' end of *CUT2* genomic DNA (see Supplemental Figure 1A online). Protoplast-mediated transformation of *M. grisea* strain Guy11 with the pPS21 plasmid yielded >90 hygromycin-resistant transformants. Of these, 89 were ectopic and/or carried multiple integrations of the pPS21 plasmid (e.g., T3 and T40; see Supplemental Figure 1B online). The single exception was transformant T41, shown by DNA gel blot analysis to be the product of a single integration event, via homologous double crossover (see Supplemental Figure 1B online). To confirm that *CUT2* disruption had resulted in gene inactivation, we showed absence of *CUT2* transcripts in epidermal strips harvested at 8 hpi from barley leaves inoculated with the *cut2* mutant strain. By contrast, *CUT2* transcripts were abundant at 8 hpi on epidermal strips inoculated with wild-type Guy11. Expression of the β -tubulin gene was consistently high in both strains (see Supplemental Figure 1C online). To ensure that the altered phenotype of the *cut2* mutant, as described below, was specifically due to gene inactivation, we complemented the *cut2* mutant by introducing the plasmid pPS22, which contains the full-length *CUT2* gene with its native promoter and terminator sequences and a selectable sulphonylurea marker (Carroll et al., 1994). One of the 29 resulting transformants was shown by PCR and DNA gel blot analysis to contain a single copy of the *CUT2* gene (data not shown) and was designated *cut2/CUT2* strain. Quantitative real-time RT-PCR analysis confirmed that the expression of the *CUT2* gene in the complemented *cut2/CUT2* strain was similar to that of Guy11 (see Supplemental Figure 1C online).

The *cut2* Mutant Shows Reduced Extracellular Cutin-Induced and Cutin-Degrading Activity

To evaluate the minimum growth requirements of the *cut2* mutant compared with wild-type Guy11 and the reconstituted strain *cut2/CUT2*, we compared growth and sporulation of the strains on selected media. Extensive but comparable hyphal radial growth and sporulation was seen for all three strains on complete (CM) or minimal medium (MM) containing glucose (see Supplemental Figure 2 online). None of the strains grew on CM or MM in the absence of glucose. All three strains grew sparsely and failed to sporulate when plant cutin was the sole carbon source in MM. Similarly, when the synthetic polyester polycaprolactone (PCL), substrate and inducer of *F. solani* cutinase (Murphy et al., 1996), or Tween 80, inducer of lipase activity (Marek and Bednarski, 1996), represented the sole carbon source, growth was sparse and colonies failed to sporulate. Addition of glucose to MM with cutin, PCL, or Tween 80 restored growth of the strains to that on MM-containing glucose.

We exploited the sparse growth of the colonies on MM with cutin to compare extracellular cutin-degrading enzyme activity. The plates were overlaid, at 10 d growth, with agarose carrying *p*-nitrophenol butyrate (PNB). A smaller yellow halo appeared in

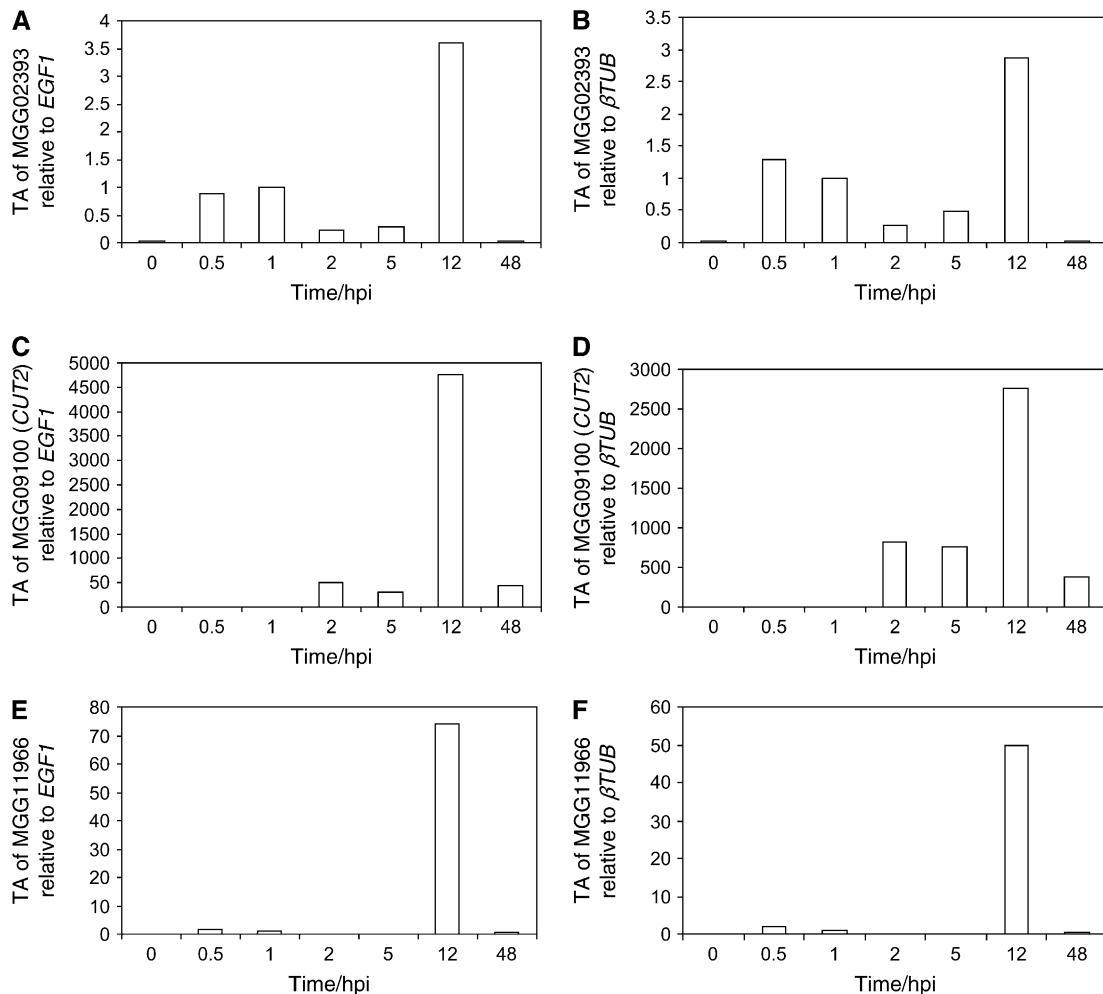


Figure 1. Transcript Analysis of Three Putative *M. grisea* Penetration-Related Cutinases in Planta.

Quantitative real-time RT-PCR monitored the relative transcript abundance (TA) of *M. grisea* Guy11 penetration-related cutinases during fungal differentiation and infection of barley leaves at 0, 0.5, 1, 2, 5, 12, and 24 hpi. Each profile was normalized independently against *EGF1* (**[A]**, **[C]**, and **[E]**) and β TUB (**[B]**, **[D]**, and **[F]**) and calibrated to 1 hpi. PCR reactions were performed in triplicate, controls with no cDNA, and no RT enzyme showed amplification.

the *cut2* mutant, compared with the larger haloes of Guy11 and *cut2*/CUT2. This provided visual evidence that *cut2* is impaired in its ability to degrade cutin when growing on cutin as the sole carbon source (see Supplemental Figure 2F online).

A more quantitative analysis of Ser esterase activity used equivalent numbers of *M. grisea* spores (4000) differentiating in hydrophobic plastic ELISA wells (inductive to appressorium formation in Guy11) in the presence of MM (with 1% glucose), MM without glucose, and MM supplemented with 0.2% cutin as sole carbon source (Table 1). The time points used for the PNB measurements in the selected media were 12 and 16 hpi (for the latter, the media were washed off at 12 hpi and replaced with fresh media for a further 4 h). No significant activity was recorded when cultures were grown without glucose, although at 16 hpi some low activity was detected. In the presence of glucose, activity levels were significantly lower in all three strains tested compared with those of cultures induced by cutin (Table 1). We

measured a statistically significant reduction in Ser esterase activity in the *cut2* mutant compared with Guy11 (~57 and ~85% of the Guy11 activity in MM at 12 and 16 hpi, respectively) and a reduction in the presence of cutin only (~66 and ~62% of the Guy11 activity in MM with cutin at 12 and 16 hpi, respectively). The high Ser esterase activity retained in the *cut2* mutant may reflect the residual cutinase activity derived from the remaining 15 putative cutinases in *M. grisea*, as seen in the *cut1* mutant (Sweigard et al., 1992b). Collectively, these data show that extracellular cutin-induced and cutin-degrading activity is reduced in the *cut2* mutant compared with the wild type and restored in the complemented strain.

Lastly, we exploited a monoclonal antibody (MAb), CD9, raised to purified cutinase from *F. solani* f. sp. *pisi* and demonstrated to recognize cutinases of *B. cinerea* and *R. solani* (Purdy and Kolattukudy, 1975; Coleman et al., 1993). The ELISA absorbance values (mean \pm SD) of 4000 germlings growing for 16 h in liquid

Table 1. Ser Esterase Activity of Guy11, *cut2*, and *cut2/CUT2* Germlings in Hydrophobic Plates (Inductive to Appressorium Formation in Guy11) with Liquid MM with 1% Glucose, MM without Glucose, and MM with 0.2% Plant Cutin as the Sole Carbon Source

Strain	MM	MM – Glucose	MM + Cutin
Guy11 (12 h)	58.3 ± 0.8	0	137.5 ± 2.4
<i>cut2</i> (12 h)	33.3 ± 0.8	0	91.6 ± 0.8
<i>cut2/CUT2</i> (12 h)	58.3 ± 2.5	ND	ND
Guy11 (16 h)	45.8 ± 0.8	8.3 ± 5.1	154.2 ± 4.6
<i>cut2</i> (16 h)	39.2 ± 2.4	12.5 ± 0.8	95.8 ± 2.4

Ser esterase activity was measured with PNB in nM min^{-1} per 1000 spores of Guy11, *cut2*, and *cut2/CUT2* at 12 hpi or at 16 hpi (after the liquid was replaced with fresh medium at 12 h and incubated for a further 4 h). Values are the average of three independent biological experiments, with each experiment consisting of three replicates and each replicate containing 4000 spores. ND, not determined.

MM supplemented with 0.2% cutin were as follows: for Guy11, 0.4 ± 0.02 ; for the *cut2* mutant, 0.36 ± 0.005 . This shows a statistically significant reduction in recognition of the anticutinase MAb in the *cut2* appressorium-stage germlings compared with Guy11 when induced by cutin ($P < 0.05$). The *cut2* mutant showed a reduced but significant absorbance value, which likely reflects residual activity from the remaining putative cutinases. The similar molecular masses of the 16-membered cutinase family precluded protein gel blot analysis.

Taking into account the results from the visual and quantitative enzyme and immunological assays, we conclude that *CUT2* encodes a secreted cutinase in *M. grisea*.

The *cut2* Mutant Phenotype Shows Reduced Conidiation and Aberrant Germling Morphology

The pyriform conidia produced by the *cut2* mutant are morphologically indistinguishable from those of the wild-type strain

Guy11. However, the number of conidia formed by the *cut2* mutant growing on solid medium for 4, 8, 12, and 16 d is reduced to ~52% of that of Guy11, ectopic transformant strain T3, and complemented strain *cut2/CUT2* (data not shown). Sexual crosses of the *cut2* mutant (Guy11 background) with the opposite mating-type strain TH3 on oatmeal agar plates gave rise to perithecia containing normal asci and ascospores. Sexual reproduction in the *cut2* mutant thus remains unaffected. Upon germination of the conidia, one, two, or three germ tubes emerged from the proximal and/or distal end cells of the three-celled conidium of the *cut2* mutant compared with a single tube seen in strain Guy11, *cut2/CUT2*, and the ectopic transformant strains T3 and T41. Scanning electron microscopy revealed that by 10 hpi on inductive hydrophobic plastic, the vast majority of *cut2* germlings had formed near straight germ tubes with either a beaded appearance and/or ending in baguette-shaped appressoria (Figure 2). By 24 hpi, the germ tube was elongated (~84 μm) with ~26% of germlings forming terminal wild-type-like appressoria (Figure 2, Table 2). The *cut2* mutant spores remained turgid at 24 hpi on plastic (Figure 2). Such characteristics contrast markedly with a single, shorter (27 μm), often curved germ tube and dome-shaped appressorium seen in wild-type Guy11, the complemented *cut2/CUT2*, and the mutant T3 strains on an inductive hydrophobic surface, which is accompanied by collapse of the conidium (Figure 2, Table 2).

Detailed scoring data revealed that on inductive hydrophobic plastic, Guy11 produced appressoria by 5 hpi (25%), and melanized appressoria were formed by 68% of germlings at 12 hpi and by 75% at 24 hpi (Figure 3A). By contrast, at 5 hpi, some 35% of mutant *cut2* germlings had appressoria; however, at 12 hpi, only 25% of germlings had developed melanized appressoria, a percentage that remained constant at 24 hpi. A high proportion of these *cut2* appressoria were unusually shaped compared with the dome-shaped wild-type appressoria or had other aberrant characteristics (e.g., abnormal appressoria with germ tubes branching off them; 13% at 24 hpi). However, the most anomalous

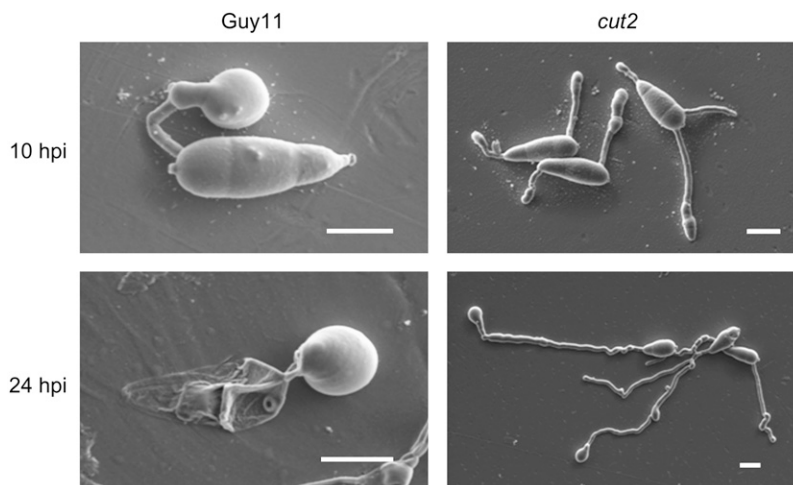


Figure 2. Scanning Electron Microscopy Images of Guy11 and the *cut2* Mutant at 10 and 24 hpi on Hydrophobic Plastic.

Bars = 10 μm .

Table 2. Appressorium Formation of *M. grisea* Guy11 and Mutant Strains *cut2*, T3, T41, and *cut2/CUT2* in Response to Various Surfaces and Pharmacological Agents

Strain	Treatment	Appressoria (%)
Guy11	Plastic	75.8 ± 10
<i>cut2</i>	Plastic	25.8 ± 7.5*
T3	Plastic	94.5 ± 3.5
T41	Plastic	96 ± 2.7
<i>cut2/CUT2</i>	Plastic	77.1 ± 8.9
Guy11	Glass	0
T3	Glass	0.33 ± 0.47
T41	Glass	0.66 ± 0.47
<i>cut2</i>	Glass	14.5 ± 6 *
<i>cut2/CUT2</i>	Glass	0
Guy11	Plastic + 1 μM diol	99.1 ± 0.8
<i>cut2</i>	Plastic + 1 μM diol	97.9 ± 0.4
Guy11	Glass + 10 μM diol	89.1 ± 2.5
<i>cut2</i>	Glass + 10 μM diol	55.8 ± 2.5**
Guy11	Plastic + 1 mM cAMP	81.6 ± 7.5
<i>cut2</i>	Plastic + 1 mM cAMP	84.1 ± 0.8
Guy11	Glass + 10 mM cAMP	57.0 ± 0.4
<i>cut2</i>	Glass + 10 mM cAMP	55.8 ± 5.8
Guy11	Plastic + 2.5 mM IBMX	81.6 ± 6.6
<i>cut2</i>	Plastic + 2.5 mM IBMX	85.8 ± 2.5
Guy11	Plastic + 20 μg/ml DAG	75.5 ± 9.2
<i>cut2</i>	Plastic + 20 μg/ml DAG	76.2 ± 11.0
Guy11	Plastic + 1 μM propranolol	76.2 ± 2.9
<i>cut2</i>	Plastic + 1 μM propranolol	59.5 ± 0.4*

The percentage of normal wild-type-like appressoria formed by the strains tested after 24 h of incubation on inductive hydrophobic plastic or noninductive hydrophilic glass surfaces, with or without the addition of pharmacological agents. Values are the mean ± SD from at least three independent experiments per treatment. In each experiment, 120 spores from a conidial suspension (10^4 mL⁻¹) of each strain were scored. Conidial germination rates were similar for each strain in all treatments. Significant differences between the percentages of appressoria formed by the *cut2* mutant relative to Guy11 and *cut2/CUT2* strains are indicated by one asterisk ($P < 0.05$) and two asterisks ($P < 0.001$).

characteristic of the *cut2* mutant was the formation of two or more elongate germ tubes, which had either swollen or hooked tips (19% at 24 hpi) or carried melanized or unmelanized appressoria (16% at 24 h). The morphologies of strains *cut2/CUT2*, T3, and T41 on plastic were not significantly altered from that of wild-type Guy11 (Table 2).

On noninductive glass, by 5 hpi, 88% of Guy11 germlings had formed elongate germ tubes but no appressoria (Figure 3B). This contrasts with the *cut2* mutant in which, at 5 hpi, ~50% of the germlings had formed single elongated germ tubes and ~23% appressoria. By 24 hpi, there was little change in Guy11, with a predominance of elongate germ tubes and an absence of appressoria, but in the *cut2* mutant, a population of appressoria (24%), of which 15% were melanized, were evident (Figure 3B). These data highlight the importance of hydrophobicity as a signal for appressorium differentiation in Guy11. They also show that the *cut2* mutant has partially lost the ability to sense the appropriateness of each surface and develop accordingly.

Cut2 Is Required for Full Plant Infection

Pathogenicity assays on blast-susceptible rice cultivar CO-39 and barley cultivar Pastoral revealed delayed disease symptoms in the *cut2* mutant. Symptoms emerged fully by 6 to 7 d after infection compared with 4 to 5 d following Guy11 infection. Furthermore, the *cut2* mutant produced only approximately one-third of the lesions caused by Guy11 on both rice and barley (Figure 4). The reduced infectivity of *cut2* on both hosts was restored in the *cut2/CUT2* reconstituted strain. Disruption of *CUT2* therefore drastically attenuated virulence but did not abolish pathogenicity. While the *cut2* mutant showed reduced plant infection, removal of the cuticle by gentle leaf abrasion prior to infection restored the speed and number of disease lesions (data not shown). Thus, the severely impaired virulence of the *cut2* mutant is due to penetration defects, whereas in planta invasive growth remains as in Guy11.

Host Penetration Is Impaired in the *cut2* Mutant, but Surface Adhesion and Appressorium Turgor Generation Are Unaffected

We asked whether the severely reduced pathogenicity of the *cut2* mutant is attributable to one or more defects at critical stages of differentiation. We reasoned that Cut2 may influence the composition of the ECM, which adheres the spore and mature appressorium to the host. We compared the adhesion of Guy11 and *cut2* spores, germ tubes, and appressoria (at 0, 2, 5, 8, 12, and 24 hpi) on hydrophobic ELISA plates using crystal violet staining in a spectrophotometric assay. We previously demonstrated that germling differentiation on this hydrophobic plastic surface is comparable to the hydrophobic plastic inductive to appressorium formation, as used in the scoring experiments (Skamnioti et al., 2007). There was no significant difference between the wild type, the *cut2* mutant, or *cut2/CUT2* at any time point, which indicates that Cut2 is unlikely to be involved in *M. grisea* adhesion. For example, at 2 hpi ~6% and at 12 hpi ~95% of the three strain germlings had adhered. Moreover, addition of 0.01, 0.05, or 0.1% SDS had no differential effect on strain adhesion at 12 hpi, with ~50, 15, and 1%, respectively, of the three strain germlings bonded to hydrophobic plastic.

We compared the spectral profiles of conidial cell walls by Raman spectroscopy, a technique that measures inelastically scattered light following excitation based on the vibrational energy levels of chemical bonds (Huang et al., 2004; Skamnioti et al., 2007). We found no differences between the strains, suggesting that the secretion of Cut2 has no effect on the integrity of the fungal cell wall.

We hypothesized that the severely reduced pathogenicity of the *cut2* mutant may be due to defective generation of appressorium turgor pressure required to breach the host cuticle. We compared cell collapse of Guy11, the *cut2* mutant, and *cut2/CUT2* appressoria in 1, 2, 3, and 4 M glycerol at 24 and 48 hpi. There was no statistically significant difference between the generated turgor pressures of the three strains. For example, at 48 hpi in 3 M glycerol, appressorial collapse was $91.7\% \pm 2.0\%$ in Guy11, $89\% \pm 3.1\%$ in *cut2*, and $90.0\% \pm 4.6\%$ in *cut2/CUT2*. We evaluated penetration peg formation in the *cut2* mutant. We

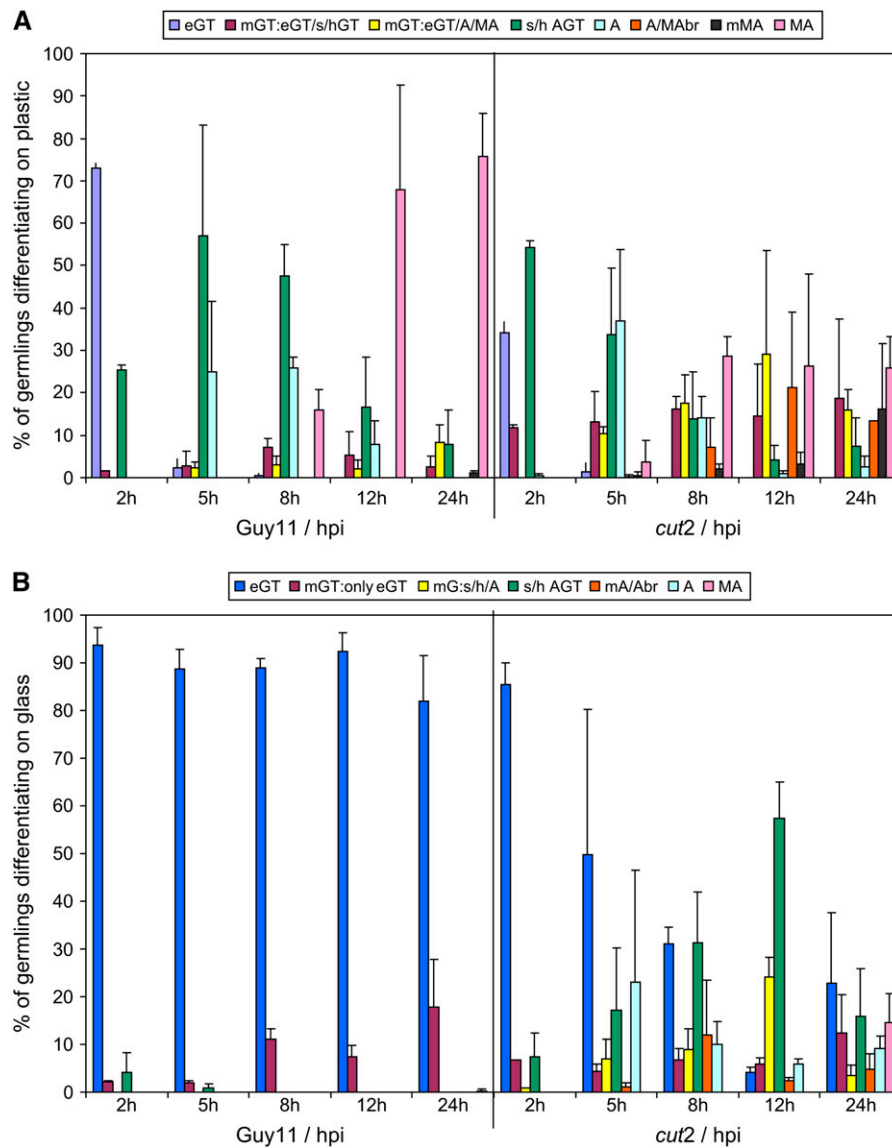


Figure 3. Morphological Phenotypes of Guy11 and *cut2* on Surfaces Inductive and Noninductive to Appressorium Formation.

M. grisea wild-type Guy11 and *cut2* mutant germling differentiation on hydrophobic plastic (inductive to appressorium formation in Guy11; **[A]**) and hydrophilic glass (noninductive; **[B]**). Germlings were scored at 2, 5, 8, 12, and 24 hpi and recorded in the following categories on plastic: eGT, elongated germ tube; mGT:eGT/s/hGT, multiple elongated tubes or germ tubes swollen or hooked; mGT, multiple germ tubes carrying appressoria and/or melanized appressoria; s/h AGT, swollen or hooked germ tube; A/MAbr, branched melanized or unmelanized appressoria; mMA, multiple melanized appressoria; MA, wild-type-like melanized appressoria. On glass, the same categories apply, with the following additions: mGT:onlyeGT, multiple elongated germ tubes; mG:s/h/A, multiple germ tubes, swollen/hooked, and/or ending in appressoria. At least three biological replicates with 120 spores each were scored per surface. Error bars represent the SD of all replicates.

found a drastically reduced number of penetration events in *cut2* ($30\% \pm 6.4\%$) compared with Guy11 ($93\% \pm 4.7\%$) and *cut2*/*CUT2* ($89\% \pm 3.8\%$) on onion epidermis at 48 hpi (Figure 5). Those penetration pegs formed, and developed into infection hyphae ramifying through intracellular tissues. These data account for the reduced disease lesions caused by *cut2* compared with the wild type and *cut2*/*CUT2*.

In conclusion, disruption of *CUT2* leads to severe inhibition of penetration events. Spore and appressorial adhesion, appres-

sorial turgor generation, and cell wall integrity remain unaffected in the mutant strain.

Surface Sensing Defects in the *cut2* Mutant: Restoration of *cut2* to Wild-Type Phenotype Levels by Cutin Monomers and Hydrophobicity

To determine whether synthetic cutin monomers are sufficient to restore to wild type the aberrant morphology of the *cut2* mutant,

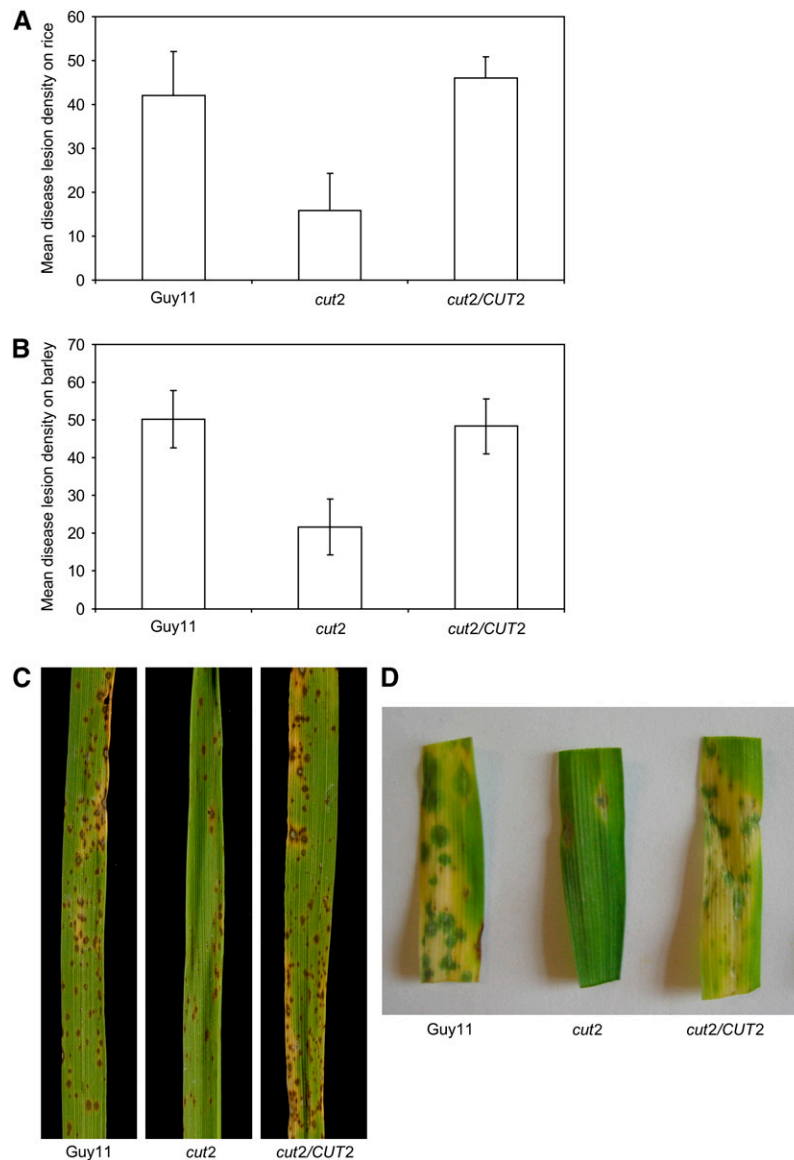


Figure 4. Pathogenicity of Guy11, *cut2*, and *cut2/CUT2* Strains on Barley and Rice.

Mean disease lesion density and typical symptoms recorded on rice **[A]** and **[C]** and barley **[B]** and **[D]** plants. Error bars represent SD. Plants were sprayed with conidial suspensions (10^4 mL⁻¹ spores) in 0.25% gelatin. Six days after inoculation, 40 randomly picked leaves were scored for the number of lesions on 5-cm leaf lengths in three independent experiments.

we exogenously applied 1,16-hexadecanediol (diol; Gilbert et al., 1996) to germlings of both strains differentiating for 24 hpi on inductive hydrophobic plastic and noninductive hydrophilic glass (Table 2). On plastic, 1 μ M diol restored *cut2* mutant appressorium formation levels to those of Guy11 (26% with no agonist; 98% with 1 μ M diol). Diol also invoked efficient appressorium formation in Guy11, rising from 76% with no agonist to 99% in the presence of 1 μ M diol. On glass, 10 μ M diol raised Guy11 appressorium formation levels from 0 to 89%. These data highlight that cutin monomers are sufficient to induce appressorium formation in the wild-type strain Guy11, even in the absence of a hydrophobic cue as observed by Gilbert et al. (1996). However,

addition of 10 μ M diol to the *cut2* mutant developing on glass led to only 56% appressorium formation, compared with 14.5% observed without the agonist. Furthermore, upon addition of diol to glass, *cut2* germling morphology resembled that of untreated *cut2* differentiating on inductive plastic surfaces. The addition of diol on noninductive surfaces therefore only partially restores wild-type morphology to the *cut2* mutant; the additional hydrophobic signal is a prerequisite for full wild-type appressorium differentiation.

We found that the addition of 1 μ M diol to equal concentrations of Guy11 and *cut2* conidial suspensions used to infect barley plants resulted in similar numbers of disease lesions (Table 3).

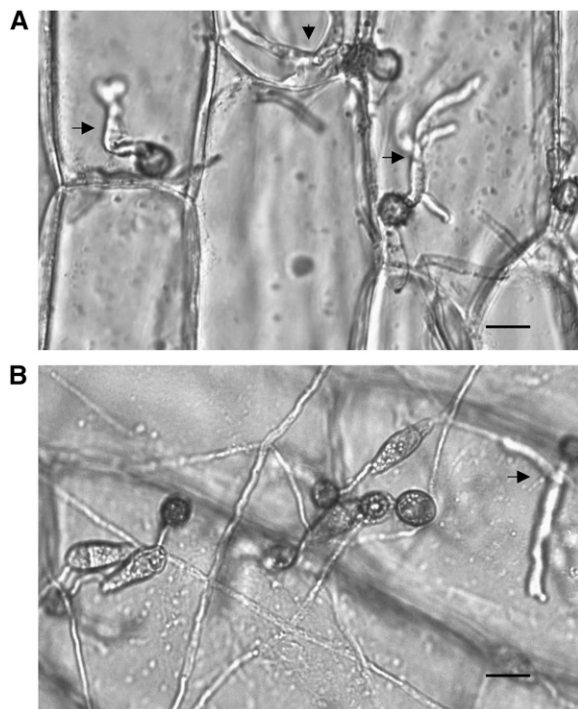


Figure 5. Visualization of Penetration Defects of *cut2* Compared with Guy11.

At least three penetration sites are visible (arrows) in onion epidermal cells inoculated 48 hpi with wild-type Guy11. By contrast, a single penetration event is seen in the *cut2* mutant. Mutant *cut2* spores remain turgid at 48 hpi, and germlings show elongated germ tubes carrying appressoria that have failed to penetrate. Bars = 10 μm .

Diol thus restores not only the morphology but also the pathogenicity of *cut2* to wild-type levels on the host plant.

Pharmacological Rescue of the *cut2* Mutant to the Wild-Type Phenotype by Exogenous cAMP, 3-Isobutyl-1-Methylxanthine, Diacylglycerol, and Propranolol

To evaluate where Cut2 lies in the signaling pathways known to induce/mediate appressorium morphogenesis, we added exogenous cAMP, 3-isobutyl-1-methylxanthine (IBMX), diacylglycerol (DAG), or propranolol to Guy11 or the *cut2* mutant and examined both germling differentiation and plant infectivity (with cAMP, IBMX, and DAG). On inductive plastic, 24 h of exposure to 1 mM cAMP resulted in restoration of the *cut2* mutant to wild-type Guy11 appressorium differentiation levels, notably rising from 26 to 84% appressorium formation in *cut2* and from 76 to 82% in Guy11 (Table 2). When 10 mM cAMP was supplemented onto noninductive glass, appressorium differentiation levels were similar in both *cut2* and Guy11 (rising to 56%), with the mutant *cut2* phenotype being restored to the phenotype displayed on plastic (Table 2). These data infer that Cut2 is likely to act in the early stages of the cAMP-induced signaling cascades of appressorium differentiation. Moreover, it further demonstrates that a hydrophobic cue cannot be overcome by exogenous cAMP

alone. To corroborate this notion, we treated germlings on plastic with exogenous IBMX, an inhibitor of cyclic nucleotide phosphodiesterase activity that downregulates the concentration of cellular cAMP. The presence of 2.5 mM IBMX suppressed the defects of appressorium morphogenesis in the *cut2* mutant relative to Guy11, forming ~ 86 and 82% appressoria, respectively (Table 2).

Activation of the PKC signaling pathway via exogenous application of 20 $\mu\text{g/mL}$ DAG to the inductive hydrophobic surface also suppressed the differentiation defects of the *cut2* phenotype, restoring it to wild-type levels (both strains showed 75% appressorium formation; Table 2). By contrast, the addition of up to 50 $\mu\text{g mL}^{-1}$ DAG to glass only partially restored appressorium formation in the *cut2* mutant (from 14 to 24%), confirming the importance of the hydrophobic signal to appressorium formation in *M. grisea*.

We added the mammalian GPCR β -adrenoreceptor antagonist propranolol to the *cut2* mutant and Guy11 germlings differentiating on inductive plastic. This adrenergic receptor has 43% sequence identity and 69% similarity with the *M. grisea* GPCR-like protein MGG05214, reported by Kulkarni et al. (2005) to carry the Pth11-CFEM domain. Propranolol had no effect on appressorium differentiation levels in Guy11, which remained constant at $\sim 76\%$. However, appressorium differentiation of the *cut2* mutant on plastic rose from 26 to 60% in the presence of propranolol. This GPCR antagonist therefore partially restored appressorium differentiation in the *cut2* mutant.

As the capacity to form normal appressoria does not necessarily lead to full virulence (Xu et al., 1998), we tested whether activation of the cAMP and/or PKC pathways in the *cut2* strain was sufficient to also restore the severely compromised infectivity of the mutant. We performed pathogenicity tests on barley

Table 3. Pathogenicity of *M. grisea* Guy11, *cut2*, and *cut2/CUT2* Strains on Barley, with or without the Addition of Pharmacological Agents

Strain	Pharmacological Agents	Pathogenicity
Guy11	–	50.2 \pm 7.6
<i>cut2</i>	–	21.6 \pm 7.4**
<i>cut2/CUT2</i>	–	48.3 \pm 7.2
Guy11	1 μM diol	54.4 \pm 7.3
<i>cut2</i>	1 μM diol	58.6 \pm 2.8
Guy11	1 mM cAMP	54.6 \pm 6.5
<i>cut2</i>	1 mM cAMP	50.0 \pm 5.7
Guy11	2.5 mM IBMX	43.4 \pm 3.1
<i>cut2</i>	2.5 mM IBMX	37.5 \pm 6.7
Guy11	20 $\mu\text{g/mL}$ DAG	39.5 \pm 5.2
<i>cut2</i>	20 $\mu\text{g/mL}$ DAG	40.8 \pm 5.1
Guy11	1 mM cAMP + 20 $\mu\text{g/mL}$ DAG	49.1 \pm 3.8
<i>cut2</i>	1 mM cAMP + 20 $\mu\text{g/mL}$ DAG	47.6 \pm 5.3

Values are the mean number of disease lesions \pm SD from two independent experiments (three in the case of no added chemicals). In each experiment, plants were sprayed with a conidial suspension (10^4 mL^{-1}) and incubated for 6 d before scoring 40 randomly picked leaves. The only statistically significant difference found between the numbers of lesions formed by *cut2* compared with Guy11 and *cut2/CUT2*, under any conditions, is highlighted with two asterisks ($P < 0.001$).

following treatment with cAMP, IBMX, or DAG, and with cAMP and DAG combined. Specifically, addition of 1 mM cAMP and 20 μ g/mL DAG applied separately or in combination or 2.5 mM IBMX in the conidial suspension of the *cut2* strain restored the speed and severity of infection of barley to levels observed with Guy11 (Table 3). The severity of disease caused by Guy11 was unchanged by drug treatment.

To further demonstrate the involvement of Cut2 in regulation of the cAMP/protein kinase A (PKA) and DAG/PKC pathways, we examined the transcript levels of particular genes known, or anticipated to play a pivotal role in these pathways, in Guy11 and the *cut2* mutant growing on barley epidermis at 8 hpi. Specifically, we chose genes encoding the catalytic subunit of protein kinase A, *cPKA* (MGG06368; Mitchell and Dean, 1995); MAP kinase 1, *PMK1* (MGG09565; Xu and Hamer, 1996); and the singleton *M. grisea* sequence encoding for an archetypal fungal PKC (MGG08689; Zhang et al., 2001). All three studied genes were significantly but variably downregulated in the mutant *cut2* strain compared with Guy11 ($P < 0.001$; Figure 6). These results collectively provide evidence that (1) secreted *M. grisea* Cut2 is an upstream activator of cAMP/PKA- and DAG/PKC-mediated

signal transduction cascades and that (2) Cut2 is pivotal to true appressorium formation and host penetration. They also hint at a potential involvement of Cut2 with a GPCR receptor.

DISCUSSION

We present genetic evidence that the *M. grisea* virulence determinant Cut2 is required for the induction of signaling pathways that lead to correct germling morphogenesis and to plant penetration. Previously, disruption of *CUT1* resulted in a fully infective strain (Sweigard et al., 1992b, 1992a), but those data did not, however, preclude involvement of other cutinases in the establishment of infection (Sweigard et al., 1992a, 1992b). The 16 putative cutinases present in the *M. grisea* genome database kindled our interest in evaluating their role in pathogenicity. We wished to establish whether cutinase aids ingress in a fungus much cited as being able to penetrate its host by mechanical force (Howard et al., 1991; reviewed in Talbot, 2003; Wang et al., 2005).

We focused on the three putative cutinases (MGG09100 [*CUT2*], MGG11966, and MGG02393) with transcripts upregulated during germling morphogenesis on artificial hydrophobic surfaces inductive to appressorium formation compared with noninductive surfaces (Dean et al., 2005; Lees et al., 2007). Interestingly, *CUT1* shows little temporal or surface-specific induced expression changes, which may explain its dispensability for infection (Sweigard et al., 1992b, 1992a); alternatively, other cutinases may compensate for the action of Cut1. Detailed in vivo transcript profiling of these genes, over seven critical developmental time points, revealed two to show a largely similar gene expression profile to that seen on artificial surfaces. However, our data revealed that the magnitude of the gene transcript changes, especially in the case of *CUT2*, was considerably greater in vivo, highlighting the responsiveness of a set of genes to the living host surface compared with artificial substrates.

The dramatic upregulation of *CUT2* during penetration in vivo led us to create a *cut2* disruption mutant, a strain displaying drastically reduced pathogenicity. Such attenuation of infectivity may hint at functional redundancy within this large family of cutinases. We discuss our findings for Cut2 in the context of the events leading from germination of the asexual spore, through germling differentiation, to plant penetration, as we demonstrated that Cut2 is not involved in *M. grisea* sexual reproduction. The *cut2* mutant produces normal pyriform conidia but with reduced levels of conidiation. However, reduced conidiation is a pleiotropic defect encountered in a variety of mutants, including *magB* (heterotrimeric G α subunit protein), *mgb1* (G β subunit), *mac1* (adenylate cyclase), and mitogen-activated protein kinase1 (*mps1*) (Xu and Hamer, 1996; Choi and Dean, 1997; Liu and Dean, 1997; Xu et al., 1998; Nishimura et al., 2003).

The ECM acts as a conduit for the exchange of signals between pathogen and plant and as an adhesive to secure the fungus to its host (reviewed in Tucker and Talbot, 2001; Carver and Gurr, 2006). Cut2, alongside other cutinases, is likely secreted in the ECM exuded from the spore or in the ring of material underpinning and firmly attaching the mature appressorium to the host during the buildup of turgor pressure needed to breach

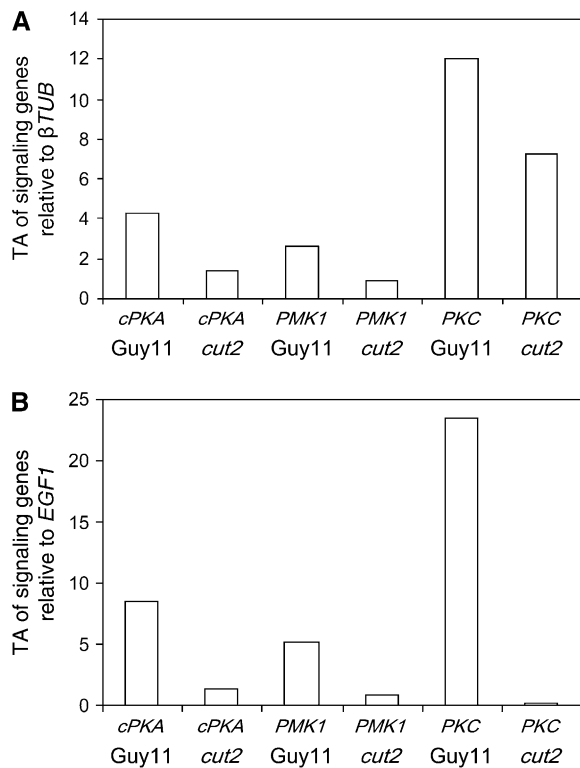


Figure 6. Transcript Analysis of Selected Signal Transduction Genes in Planta.

Quantitative real-time RT-PCR monitored the relative transcript abundance (TA) of *M. grisea* *cPKA*, *PMK1*, and *PKC* genes in wild-type Guy11 and *cut2* strains at 8 hpi on barley leaves. Each profile was normalized independently against β TUB (A) and EGF1 (B). PCR reactions were performed in triplicate, controls with no cDNA, and no RT enzyme showed no amplification.

the cuticle (Howard et al., 1991). We found visual evidence for reduced extracellular cutin-degrading activity in *cut2* grown on cutin as sole carbon source compared with Guy11 and *cut2/CUT2*. More refined and quantitative sampling of culture filtrates, again grown in presence of cutin alone, showed that *cut2* appressorium-stage germlings had approximately two-thirds of the Ser esterase activity of either wild-type Guy11 or *cut2/CUT2*. Furthermore, ELISA assays with MAb CD9, raised to *F. solani* f. sp. *pisii* cutinase (Purdy and Kolattukudy, 1975; Coleman et al., 1993), showed reduced recognition of an anticutinase MAb in the *cut2* mutant compared with wild-type Guy11. We found no evidence, however, that Cut2 contributes significantly to adhesion at any stage of germling differentiation on the plant. Therefore, it is unlikely that Cut2 plays the role demonstrated for the cutinases of *U. viciae-fabae* (Deising et al., 1992), or proposed for other fungi (Pascholati et al., 1992, 1993), or akin to the *M. grisea* hydrophobins Mpg1 and Mhp1 (Talbot et al., 1993, 1996; Kim et al., 2005).

The events of the initial recognition phase, where the suitability of the substrate is monitored (Bourett and Howard, 1990; Howard and Valent, 1996), are greatly altered in the *cut2* mutant compared with the wild-type strain Guy11. On glass, which fails to support appressorium formation in Guy11, a small population of *cut2* germlings progress to form melanized appressoria. These data show that the mutant cannot accurately discriminate between a noninductive and an inductive surface in that *cut2* partially bypasses the need for the hydrophobic recognition cues seen with Guy11 (Gilbert et al., 1996; reviewed in Tucker and Talbot, 2001). On hydrophobic plastic inductive to appressorium formation in Guy11, *cut2* displays an aberrant morphology; it forms extremely elongated germ tubes, many of which carry multiple misformed appressoria. Only a small population of *cut2* germlings progress to form terminal, wild-type-like appressoria, attesting to its residual need for a hydrophobic signal. However, the addition of hexadecanediol to the noninductive surface demonstrated that the *cut2* mutant still requires hydrophobicity for full restoration of its morphology and pathogenicity. This anomalous boost in the number of *cut2* mutant germ tubes and appressoria on all substrates but lack of efficient penetration peg formation on inductive surfaces suggests that Cut2 is acting as an activator of differentiation and penetration in response to inductive surfaces and a partial repressor of differentiation on noninductive surfaces in the wild type, as proposed for Pth11 (DeZwaan et al., 1999).

Our data are consistent with a role for Cut2 in sensing both chemical and physical cues to evaluate the appropriateness of the host. The complex phenotype of the *cut2* mutant on artificial surfaces attests to the critical requirement for accurate integration of the signaling pathways triggered by both cutin monomers and hydrophobicity. On a suitable substrate, these cues are then transduced, through as yet unknown receptors, into intracellular signaling pathways, such as cAMP/PKA, MAP kinase, and DAG/PKC, which mediate appressorium formation, penetration, and infectious growth (reviewed in Talbot, 2003). We monitored the effect of cAMP signal transduction agonists on germling morphogenesis of the *cut2* mutant and wild-type Guy11 on inductive and noninductive surfaces. This showed that exogenous cAMP restores *cut2* appressorium formation to levels seen in Guy11 on

plastic and to wild-type levels when applied to glass. Such mutant defect suppression bears some similarity to the restoration of appressorium formation by exogenous cAMP in the *M. grisea* mutants *mac1* (Choi and Dean, 1997), *mpg1* (Talbot et al., 1993), *pth11* (DeZwaan et al., 1999), *G α magB* (Liu and Dean, 1997), *mgB1* (Nishimura et al., 2003), and *cPKA* (Xu et al., 1997). Data derived from treatment with the phosphodiesterase inhibitor IBMX also show restoration of *cut2* appressorium formation to levels seen in the wild-type strain Guy11 on plastic. By contrast, IBMX treatment did not restore appressorium formation but reduced germination in the *mac1* and *cPKA* mutants (Mitchell and Dean, 1995; Choi and Dean, 1997; Xu et al., 1997). Some support for a role for Cut2 in the activation of cAMP/PKA signaling was seen in the twofold downregulation of *cPKA* transcripts in the *cut2* mutant compared with Guy11. However, the transcript level changes are modest and merit a more detailed appraisal.

The involvement of a DAG-activated PKC pathway is implicated in the early stages of appressorium differentiation (Thines et al., 1997b; DeZwaan et al., 1999) and in crosstalk with the PKA signaling system (DeZwaan et al., 1999). We demonstrated that exogenous application of DAG restores correct germling development, appressorium formation, and pathogenicity in the *cut2* mutant. DAG also defect suppressed the *pth11* mutant by boosting appressorium formation, but less effectively than in the *cut2* mutant. However, DAG did not restore pathogenicity in *pth11* (DeZwaan et al., 1999). It is logical to assume that pathogenicity may be regulated by more than one PKC in *M. grisea*. Indeed, the genome database reveals five PKC-like sequences (<http://www.broad.mit.edu/annotation/>). Of these, MGG08689 aligns most closely with *B. graminis* *Pkc-1* (Zhang et al., 2001) and carries several hallmark features of fungal PKCs, including a putative phorbol ester/DAG binding domain. Indeed, the transcript of this gene, named *PKC*, was significantly downregulated in the *cut2* mutant, relative to Guy11. Collectively, these data attest to Cut2 operating upstream of the cAMP/PKA and DAG/PKC signal transduction response pathways in *M. grisea*.

The GPCR concept and the vital role of G-proteins in signal transduction processes stems largely from mammalian research (reviewed in Hill, 2006; Murphy et al., 2006). In our hunt for a link between Cut2 and GPCRs in *M. grisea*, we used the lipophilic mammalian GPCR β -adrenoreceptor antagonist propranolol. Curiously, we found that propranolol partially restores appressorium formation levels of the *cut2* mutant differentiating on inductive plastic to levels similar with the wild-type strain Guy11. While the data hint at some interplay between Cut2 and GPCRs, at this stage we can only hypothesize that one of the 61 Pth11-like GPCR receptors in *M. grisea* (Kulkarni et al., 2005) perceives the cutin monomer ligand, which in turn invokes an R* conformational change of bound heterotrimeric G-proteins. Heterotrimeric G-proteins, like G α and G β units (Liu and Dean, 1997; Nishimura et al., 2003), could thus relay the surface recognition signals released by Cut2, setting in motion the signal transduction pathways, and so effecting appressorium and penetration peg formation. Further support of this link is seen in the morphology of the *cut2* mutant; that is, the arrest of the germ tube tip growth, resulting in long and straight germ tubes, which is reminiscent of those seen in the *magB*, *mgB1*, and the vast

majority of the *pth11* mutants (Liu and Dean, 1997; DeZwaan et al., 1999; Nishimura et al., 2003). Furthermore, the baguette-shaped appressoria initials formed by *cut2* resemble the morphology of appressoria in the G β subunit mutant *mgb1*, as induced in the presence of cAMP (Nishimura et al., 2003).

Although most *cut2* mutant appressoria are deformed, melanization proceeds normally and turgor generation in the *cut2* mutant reaches wild-type levels. This contrasts with the complete inability to form appressoria observed for the *mac1* mutant (Choi and Dean, 1997). It thus appears that cutin monomers putatively released by Cut2 are insufficient for the generation of the cAMP signal, as the presence of a hard surface and hydrophobicity are also required (Lee and Dean, 1994; Gilbert et al., 1996; Dean, 1997). However, these chemical cues are essential for correct regulation of the cAMP signal. Furthermore, *cut2* mutant appressoria do not produce penetration pegs efficiently; penetration events and consequent disease lesions occur at only one-third of the frequency seen in wild-type Guy11. A penetration defect is also seen in the *magB* (Liu and Dean, 1997), *mgb1* (Nishimura et al., 2003), *mgs1* (Xu et al., 1998), *pls1* (Clergeot et al., 2001), and *mst12* mutants (Park et al., 2004). These data further suggest Cut2 involvement in the cAMP/PKA pathway and in the MAP kinase cascade. They also add to the body of data that attests to turgor generation and appressorium peg formation as being genetically distinct processes in *M. grisea* (Dixon et al., 1999; Park et al., 2004; reviewed in Wang et al., 2005).

Finally, the *cut2* mutant shows unaltered invasive hyphal growth (after leaf abrasion). These data suggest that Cut2 is not markedly involved during in planta intracellular growth of *M. grisea*. This contrasts with the need for cutinases during subcuticular plant growth of *V. inaequalis* (Koller et al., 1991). However, a role for Cut2, or indeed for any one of the remaining 15 cutinases in planta, cannot be dismissed, as the transcription of *CUT2* is elevated some 500-fold in *M. grisea*-infected plant tissues at 48 hpi. Indeed, a role for cutinases during infection hyphae growth through leaf tissues or during conidiophore emergence through the cuticle, as proposed by Sweigard et al. (1992b), merits further study.

The unprecedented and complex phenotype of the *cut2* mutant suggests that Cut2 plays a pivotal role in substrate sensing and signal relay in *M. grisea*. Cut2 thus ensures correct morphogenesis on the host leaf. Moreover, we have shown that while *M. grisea* mechanically breaches its host, it also invokes the cutinase Cut2 to effect full penetration through the outermost defensive barrier of the plant. We hypothesize that Cut2 is sensed by one or more cell surface receptors and thus provides the signal for the induction of multiple, integrated, or parallel signaling cascades. The putative GPCR(s) involved would form an excellent target site for the rational design of fungicides, which could effectively block the perception of host-derived signals in the rice blast fungus.

METHODS

Fungal Strains, Growth Conditions, and Nucleic Acid Analyses

The wild-type rice pathogenic *Magnaporthe grisea* strain Guy11 was used throughout this work. Strain maintenance, composition of media, DNA

and RNA extraction, and DNA-mediated transformation protocols were as described by Talbot et al. (1993). Standard procedures were adopted for restriction enzyme digestion, gel electrophoresis, DNA gel blot hybridizations, and DNA sequencing (Sambrook and Russell, 2001). CM and MM were prepared in the absence of glucose and supplemented with sole carbon sources of 1% glucose, 0.2% cucurbit cutin (Crowhurst et al., 1997), 0.1% Tween 80, and 500 mg L⁻¹ PCL (Cellomer Associates), prepared as by Murphy et al. (1996). The plates were inoculated with 4-mm-diameter agar plugs from wild-type Guy11, *cut2* mutant, or *cut2*/CUT2 colonies and incubated at 24°C for 10 d, with a 12-h light-dark cycle and five replicate plates per treatment. Mating assays were with strain TH3 (a gift from N. Talbot, Exeter University). Perithecia and ascospore formation were followed by crossing the *cut2* mutant (Guy11 background) with the opposite mating type strain TH3. Agar plug inocula of the two strains were placed 4 cm apart on oatmeal agar and incubated under constant fluorescent light at 18°C for 28 d. Perithecia were gently crushed to reveal asci and ascospores.

Quantitative Real-Time RT-PCR Transcript Profiling

Stage-specific biological material for RNA extraction was collected from *M. grisea* strain Guy11 at 0, 0.5, 1, 2, 5, 12, and 48 hpi of detached barley (*Hordeum vulgare*) leaves, essentially as described by Skamnioti et al. (2007). Considerable care was taken to monitor the timing of stage-specific germling development on barley so as to synchronize maturation of appressoria and subsequent penetration events. We used barley because we were able to routinely peel off the adaxial barley epidermal strips and use the inoculated abaxial epidermal layer in RNA preparations, thereby reducing the plant component; rice epidermal peels proved problematic. First-strand cDNA was synthesized from total RNA using the RETROscript first-strand synthesis kit (Ambion). Real-time PCR was performed on first-strand cDNAs, prepared as above, using the QuantiTect SYBR green RT-PCR kit (Qiagen). Primers were designed to amplify ~100 bp and to bridge introns of cutinase genes MGG09100, MGG11966, and MGG02393. Transcript abundance of the target genes, relative to the constitutively expressed normalizer gene, β -tubulin (*β TUB* [MG00604]), was quantified, taking account of primer efficiencies as described by Pfaffl (2001). A second constitutive control gene, elongation factor1 (*EGF1* [MGG03641]) was also used as an independent normalizer. Expression analyses of MGG09100 (*CUT2*), MGG06368 (*cPKA*), MGG08689 (*PKC*), and MGG09565 (*PMK1*) in Guy11, *cut2*, and *cut2*/CUT2 strains were performed at 8 hpi with the respective strains onto detached leaves. The forward (F) and reverse (R) primers were as follows: MGG00604, F 5'-CTCTGCCATCTTCCGTGGA-3' and R 5'-ACG-AAGTACGACGAGTTCTTGTCT-3'; MGG03641, F 5'-CCTGTACC-AAGGAGCGTTAGG-3' and R 5'-TCAACGGTGACCACATGATCTC-3'; MGG11966, F 5'-acgtccccgggtcctgtta-3' and R 5'-gccaccttcgcatggtt-3'; MGG09100, F 5'-ggatgcaaggacgtcgttct-3' and R 5'-ggttct-ggcccatgtt-3'; MGG02393, F 5'-GCTTCCGGGTCGTCCAA-3' and R 5'-ACCTTTGTTCTGGGCATTTT-3'; MGG06368, F 5'-CCAACGACGA-GCGCAA-3' and R 5'-CAACGTAATCAGAACGGATTCT-3'; MGG09898, F 5'-TTGACGACCTGGAGGAATACAGT-3' and R 5'-TTGGTGAATT-TGTTGCAGTTGAT-3'; MGG08689, F 5'-GGAAGACATGTGGTACGG-CTCTA-3' and R 5'-GCAAAATTTCTGGTCCATAAAC-3'; MGG09565, F 5'-GCCAGGGCGCTTATGGA-3' and R 5'-TCITCTTTATGGCAACCTTT-TGG-3'.

Real-time quantification was performed using the ABI Prism 7300 sequence detection systems (Applied Biosystems), cycling 50°C, 2 min, 1 cycle; 95°C 10 min 1 cycle; 95°C 15 s, 60°C 1 min, 40 cycles. Reactions with no cDNA added (no template controls) monitored for the presence of primer dimers and no reverse transcriptase controls (-RTs) were included for each cDNA sample. PCRs were performed in triplicate and mean values determined.

Targeted Gene Replacement of *M. grisea* *CUT2* and Complementation of the *cut2* Mutant

The full-length MGG09100 (*CUT2*) gene and its 1842-bp upstream and 1012-bp downstream flanking sequences were amplified by PCR and cloned into the *EcoRI* site of pGEM-T-easy (Stratagene) to form plasmid pPS20. Digestion of pPS20 with *XhoI* released a 93-bp fragment located at the end of the 5'-untranslated region, including the first 63 bp of the *CUT2* gene sequence. This was replaced by the *Sall*-hygromycin B resistance gene (1.4 kb) released from plasmid pCB1636 (Xu et al., 1997), forming the *CUT2* disruption plasmid pPS21, which was sequence verified. Protoplast-mediated transformation of *M. grisea* Guy11 was performed following the method of Talbot et al. (1993). To confirm *CUT2* disruption, *HindIII*-digested genomic DNA from hygromycin-resistant, putative *CUT2* transformants was gel blotted on Nylon⁺ membrane (Amersham) and hybridized with a 395-bp fragment from the 3'-end of the Guy11 *CUT2* gene, which was labeled with the DIG High Prime DNA labeling and detection kit II according to the manufacturer's instructions (Roche). To assess whether a single integration event had occurred, DNA from the Guy11 and *cut2* mutants was digested with *HindIII*, gel blotted, and hybridized to the 1.4-kb hygromycin B gene amplified from pCB1632. For complementation of the *cut2* mutant, a 2885-bp *Sall*-*HindIII* fragment (which spans and overruns the *cut2* locus by 1374 and 401 bp at the 5'- and 3'-ends, respectively) was excised from pPS20 and ligated into *Sall*-*HindIII*-digested pCB1532, which carries the sulphonylurea resistance selectable marker (Carroll et al., 1994). The resulting plasmid, pPS22, was sequence verified and reintroduced into the *cut2* mutant, with transformants selected on 100 $\mu\text{g mL}^{-1}$ chlorimuron ethyl (gift from Jim Sweigard, DuPont, Wilmington, DE). The *cut2* complemented strain was designated *cut2/CUT2*.

Cutinase Induction, Enzyme Assays, and ELISA

Cutinase induction plate assays were with Guy11, *cut2* mutant, and *cut2/CUT2* strains grown on MM (no glucose) supplemented with 0.2% (w/v) cucurbit cutin. After incubation at 24°C for 10 d, the cultures were overlaid with 0.8% low melting point agarose in 50 mM sodium phosphate buffer, pH 8, containing 1.5 mM PNB, and incubated at room temperature for 30 min. Ser esterase activity was determined by measuring the rate of hydrolysis of PNB, at pH 8, by 100 μL of spore suspensions of 10-d cultures at 4×10^4 spores mL^{-1} placed in 96-well ELISA plates (hydrophobic polystyrene; Sterilin) and activity determined in (1) spores developing in MM \pm 1% (w/v) glucose or with 0.2% cutin (w/v) at 12 hpi and (2) spores developing in MM \pm 1% (w/v) glucose or 0.2% (w/v) cucurbit cutin for 12 h, whereupon the 100 μL culture supernatant was replaced with fresh medium and incubated for 4 h (16 hpi). This experiment was designed to optimize our ability to compare cutinase activity by focusing on enzymes produced specifically during maturation of the appressorium. The samples were incubated for the prescribed number of hours in a high-humidity chamber at 24°C and Ser esterase activity determined as described by Francis et al. (1996). Assays were performed in triplicate in three independently replicated experiments.

ELISA assays were performed with a MAB, CD9, raised against purified cutinase from *Fusarium solani* f. sp. *pisii*, as recorded by Coleman et al. (1993). Germlings were prepared (4000 per well) as for 16 hpi in Ser esterase assay in 0.2% (w/v) cutin. At 16 hpi, 100 μL of culture supernatant was removed to a NUNC maxisorb ELISA plate (Fisher Scientific) and the plates washed three times in PBST containing PBS (0.8% NaCl, 0.02% KCl, 0.115% Na_2HPO_4 , and 0.02% KH_2PO_4 , pH 7.2) plus 0.05% (v/v) Tween 20 (polyoxy-ethylene sorbitan monolaurate; Sigma-Aldrich). The wells were coated with 100 μL of undiluted MAB CD9 (Coleman et al., 1993) and incubated at 37°C for 1 h. The plates were washed three times in PBST. Anti-mouse polyvalent immunoglobulin peroxidase conjugate (A0412; Sigma-Aldrich) was diluted 1 in 1000 with PBST and 100 μL

added per well. Plates were washed three times in PBST and 100 μL of prewarmed TMB (tetramethylbenzidine; Adgen) substrate added to each well and plates incubated at room temperature for 5 min. Concentrated H_2SO_4 (100 μL) was added to each well and absorbance values recorded at 405 nm on an MRX automated microplate reader (Dynatech). Assays were performed in triplicate in three independent biological experiments.

Pathogenicity and Infection-Related Morphogenesis Assays

Plant infection assays were performed on blast-susceptible, 14-d-old seedlings of rice (*Oryza sativa*) cultivar CO-39 or 7-d-old seedlings of barley cultivar Pastoral. A suspension of conidia (10^4 mL^{-1}) in 0.25% (w/v) gelatin water was applied using an artist's airbrush with high-pressure air from a Kenair duster (Kenro) as described by Talbot et al. (1993). Disease lesions were counted from 40 randomly chosen 5-cm leaf tips as described by Valent et al. (1991) in three independent experiments. Mean disease lesion densities were calculated and compared. Cuticle penetration was assessed by scoring the frequency with which appressoria formed penetration pegs on onion epidermis after incubation for 24 h at 24°C. One hundred appressoria were scored in three independently replicated experiments.

Infection-related appressorium development was assessed by following germling differentiation and appressorium formation on hydrophobic plastic cover slips and hydrophilic glass slides (held at high humidity at 24°C at 2, 5, 8, 12, and 24 hpi) by counting 120 germlings in three independent experiments by light microscopy. Infection-related appressorium differentiation assays in the presence of various cAMP/PKA or DAG/PKC pathway agonists were as described above but in the presence of 1 or 10 mM cAMP (Sigma-Aldrich) from a 100 mM aqueous stock, 2.5 mM IBMX (Sigma-Aldrich) from a 0.25 M solution in 99% ethanol, 20 $\mu\text{g mL}^{-1}$ DAG (Sigma-Aldrich) from a 2.5 mg mL^{-1} solution in DMSO, 1 or 10 μM 1,16-hexadecanediol from 0.1 M stock solution in 99% ethanol, and 1 μM \pm propranolol HCl (Sigma-Aldrich) from a 10 mM solution in DMSO.

Scanning electron microscopy was undertaken by inoculating hydrophobic plastic for 10 or 24 h (at 24°C, high humidity) and the slides mounted on copper stubs at room temperature using Leit C carbon conductive cement. The stubs were rapidly inserted under a stream of dry argon into precooled stub holders (at -186°C) withdrawn from the SP2000A sputter-cryo system. The sample was introduced to the cold stage of a JEOL JSM840A scanning electron microscope at approximately -150°C to inspect for frost. No serious frosting was observed, and samples were returned to the sputter-cryo system and after recoiling to -186°C , coated with gold/palladium under argon. The samples were returned to the scanning electron microscope and digital images acquired using SemAfore.

Raman spectroscopy was performed using a LabRAM 300 microscope (Jobin-Yvon). Scattering was excited by a frequency-doubled 532-nm Nd:YAG laser. Conidia from 10-d-old plate cultures of *M. grisea* strains of the *cut2* mutant and Guy11 were harvested, filtered through two layers of Miracloth, pestle and mortar ground to a fine powder in 20 mM Tris 50 mM EDTA, pH 8, in liquid nitrogen, centrifuged at 3000g for 10 min, and lyophilized. Ten microliters were spread on a quartz slide and targeted by confocal optics. Spectra were acquired between 544 and 1972 cm^{-1} at \sim 5 to 8 mW for 60 to 90 s for three samples of each preparation, baseline corrected, normalized by Labspec software (Jobin-Yvon), and imported into MVSP 3.12d (Kovach Computing) and MatlabR12 (Math Works) for multivariate analysis.

Adhesion assays were performed based on O'Toole et al. (1999) by inoculating 100 μL of spores ($4 \times 10^4 \text{ mL}^{-1}$) into individual wells of 96-well ELISA plates (Sterilin) at 0, 2, 5, 8, 12, and 24 h and the plate incubated in a high-humidity chamber at 24°C. The plates were washed three times by tapping out the contents of the wells and submerging the wells in sterile distilled water. The plates were air dried, and 100 μL of 0.05% (w/v)

crystal violet (Sigma-Aldrich) was added to each well and incubated at room temperature for 20 min. The plates were again washed three times in sterile distilled water and air dried and 100 μ L of 98% ethanol added to each well. The plate was gently shaken at room temperature for 15 min and the absorbance of the plate measured spectrophotometrically at 570 nm. Assays were performed in triplicate in three independently replicated experiments.

Appressorium turgor was assessed by a cell collapse assay (Dixon et al., 1999). Germlings differentiating in water droplets on hydrophobic cover slips were left for 24 or 48 h under high-humidity conditions. The water was replaced by 0, 1, 2, 3, or 4 M glycerol and the germlings incubated for 10 min. Approximately 300 appressoria were scored for cell collapse per treatment in three independently replicated experiments.

Accession Numbers

Sequence data from this article can be found in the GenBank/EMBL data libraries under accession numbers MGG03641, MGG00604, MGG09100, MGG02393, MGG11966, MGG06368, MGG08689, MGG09898, and MGG09565.

Supplemental Data

The following materials are available in the online version of this article.

Supplemental Figure 1. Targeted Gene Disruption and Complementation of *M. grisea* CUT2.

Supplemental Figure 2. Growth Assays of *M. grisea* Strains on Various Media.

Supplemental Table 1. Genes Predicted to Encode Cutinases in the Genome of *M. grisea*.

ACKNOWLEDGMENTS

This work was supported by a grant to S.J.G. from the Biotechnology and Biological Sciences Research Council to specifically support P.S. We thank Zena Robinson (University of Oxford) for her expert technical assistance, Wei Huang (Centre for Hydrology and Ecology, Oxford, UK) for his help with the Raman spectroscopy, Barry Thomas and Tim Carver (Institute of Grassland and Environmental Research, Aberystwyth) for their help with the scanning electron microscopy images, Matt Templeton (Horticulture and Food Research Institute, Auckland, NZ) for the gift of cucurbit cutin, and Molly Dewey (University of Oxford) for MAb CD9. We also thank Ralph Dean (North Carolina State University, Raleigh) for discussion on cutinases, Stephen Hill (University of Nottingham Medical School, Nottingham, UK) for advice on PCRs, and Mary Illes, Gail Preston (University of Oxford), and Jesse Alderson (University of Oxford) for their critical appraisal of the manuscript.

Received February 20, 2007; revised July 17, 2007; accepted July 30, 2007; published August 17, 2007.

REFERENCES

- Adachi, K., and Hamer, J.E. (1998). Divergent cAMP signaling pathways regulate growth and pathogenesis in the rice blast fungus *Magnaporthe grisea*. *Plant Cell* **10**: 1361–1373.
- Bechinger, C., Giebel, K.F., Schnell, M., Leiderer, P., Deising, H.B., and Bastmeyer, M. (1999). Optical measurements of invasive forces exerted by appressoria of a plant pathogenic fungus. *Science* **285**: 1896–1899.
- Bessire, M., Chassot, C., Jacquat, A.-C., Humphry, M., Borel, S., MacDonald-Comber Petetot, J., Metraux, J.-P., and Nawrath, C. (2007). A permeable cuticle in *Arabidopsis* leads to a strong resistance to *Botrytis cinerea*. *EMBO J.* **26**: 2158–2168.
- Bourett, T.M., and Howard, R.J. (1990). *In vitro* development of penetration structures in the rice blast fungus *Magnaporthe grisea*. *Can. J. Bot.* **68**: 329–342.
- Carroll, A.M., Sweigard, J.A., and Valent, B. (1994). Improved vectors for selecting resistance to hygromycin. *Fungal Genetics Newsletter* **41**: 22.
- Carver, T.L.W., and Gurr, S.J. (2006). Filamentous fungi on plant surfaces. In *Annual Plant Reviews: Biology of the Plant Cuticle*, M. Riederer, ed (Oxford, UK: Blackwell Publishing), pp. 368–392.
- Chasan, R. (1992). Cutinase: Not a weapon in fungal combat. *Plant Cell* **4**: 617–618.
- Chassot, C., Nawrath, C., and Metraux, J.P. (2007). Cuticular defects lead to full immunity to a major plant pathogen. *Plant J.* **49**: 972–980.
- Choi, W.B., and Dean, R.A. (1997). The adenylate cyclase gene MAC1 of *Magnaporthe grisea* controls appressorium formation and other aspects of growth and development. *Plant Cell* **9**: 1973–1983.
- Clergeot, P.H., Gourgues, M., Cots, J., Laurans, F., Latorse, M.P., Pepin, R., Tharreau, D., Notteghem, J.L., and Lebrun, M.H. (2001). *PLS1*, a gene encoding a tetraspanin-like protein, is required for penetration of rice leaf by the fungal pathogen *Magnaporthe grisea*. *Proc. Natl. Acad. Sci. USA* **98**: 6963–6968.
- Coleman, J.O.D., Hiscock, S.J., and Dewey, F.M. (1993). Monoclonal antibodies to purified cutinase from *Fusarium solani* f. sp. *pisi*. *Physiol. Mol. Plant Pathol.* **43**: 391–401.
- Crowhurst, R.N., Binnie, S.J., Bowen, J.K., Hawthorne, B.T., Plummer, K.M., Rees-George, J., Rikkerink, E.H.A., and Templeton, M.D. (1997). Effect of disruption of a cutinase gene (*cutA*) on virulence and tissue specificity of *Fusarium solani* f. sp. *cucurbitae* race 2 toward *Cucurbita maxima* and *C-moschata*. *Mol. Plant Microbe Interact.* **10**: 355–368.
- Dean, R.A. (1997). Signal pathways and appressorium morphogenesis. *Annu. Rev. Phytopathol.* **35**: 211–234.
- Dean, R.A., et al. (2005). The genome sequence of the rice blast fungus *Magnaporthe grisea*. *Nature* **434**: 980–986.
- Deising, H., Nicholson, R.L., Haug, M., Howard, R.J., and Mendgen, K. (1992). Adhesion pad formation and the involvement of cutinase and esterases in the attachment of uredospores to the host cuticle. *Plant Cell* **4**: 1101–1111.
- deJong, J.C., McCormack, B.J., Smirnov, N., and Talbot, N.J. (1997). Glycerol generates turgor in rice blast. *Nature* **389**: 244–245.
- DeZwaan, T.M., Carroll, A.M., Valent, B., and Sweigard, J.A. (1999). *Magnaporthe grisea* Pth11p is a novel plasma membrane protein that mediates appressorium differentiation in response to inductive substrate cues. *Plant Cell* **11**: 2013–2030.
- Dickman, M.B., Podila, G.K., and Kolattukudy, P.E. (1989). Insertion of cutinase gene into a wound pathogen enables it to infect intact host. *Nature* **342**: 446–448.
- Dixon, K.P., Xu, J.R., Smirnov, N., and Talbot, N.J. (1999). Independent signaling pathways regulate cellular turgor during hyperosmotic stress and appressorium-mediated plant infection by *Magnaporthe grisea*. *Plant Cell* **11**: 2045–2058.
- Francis, S.A., Dewey, F.M., and Gurr, S.J. (1996). The role of cutinase in germling development and infection by *Erysiphe graminis* f. sp. *hordei*. *Physiol. Mol. Plant Pathol.* **49**: 201–211.
- Gilbert, M.J., Thornton, C.R., Wakley, G.E., and Talbot, N.J. (2006). A P-type ATPase required for rice blast disease and induction of host resistance. *Nature* **440**: 535–539.

- Gilbert, R.D., Johnson, A.M., and Dean, R.A. (1996). Chemical signals responsible for appressorium formation in the rice blast fungus *Magnaporthe grisea*. *Physiol. Mol. Plant Pathol.* **48**: 335–346.
- Hamer, J.E., Howard, R.J., Chumley, F.G., and Valent, B. (1988). A mechanism for surface attachment in spores of a plant pathogenic fungus. *Science* **239**: 288–290.
- Hill, S.J. (2006). G-protein-coupled receptors: Past, present and future. *Br. J. Pharmacol.* **147**: S27–S37.
- Howard, R.J., Ferrari, M.A., Roach, D.H., and Money, N.P. (1991). Penetration of hard substrates by a fungus employing enormous turgor pressures. *Proc. Natl. Acad. Sci. USA* **88**: 11281–11284.
- Howard, R.J., and Valent, B. (1996). Breaking and entering: Host penetration by the fungal rice blast pathogen *Magnaporthe grisea*. *Annu. Rev. Microbiol.* **50**: 491–512.
- Huang, W.E., Griffiths, R.I., Thomson, I.P., Bailey, M.J., and Whiteley, A.S. (2004). Raman microscopic analysis of single microbial cells. *Anal. Chem.* **76**: 4452–4458.
- Kamamura, T., Yamaguchi, S., Saitoh, K., Teraoka, T., and Yamaguchi, I. (2002). A novel gene, *CBP1*, encoding a putative extracellular chitin-binding protein, may play an important role in the hydrophobic surface sensing of *Magnaporthe grisea* during appressorium differentiation. *Mol. Plant Microbe Interact.* **15**: 437–444.
- Kim, S., Ahn, I.P., Rho, H.S., and Lee, Y.H. (2005). *MHP1*, a *Magnaporthe grisea* hydrophobin gene, is required for fungal development and plant colonization. *Mol. Microbiol.* **57**: 1224–1237.
- Kolattukudy, P.E. (1985). Enzymatic penetration of the plant cuticle by fungal pathogens. *Annu. Rev. Phytopathol.* **23**: 223–250.
- Kolattukudy, P.E., Li, D.X., Hwang, C.S., and Flaishman, M.A. (1995a). Host signals in fungal gene-expression involved in penetration into the host. *Can. J. Bot.* **73** (suppl.): S1160–S1168.
- Kolattukudy, P.E., Rogers, L.M., Li, D.X., Hwang, C.S., and Flaishman, M.A. (1995b). Surface signaling in pathogenesis. *Proc. Natl. Acad. Sci. USA* **92**: 4080–4087.
- Koller, W., Parker, D.M., and Becker, C.M. (1991). Role of cutinase in the penetration of apple leaves by *Venturia inaequalis*. *Phytopathology* **81**: 1375–1379.
- Koller, W., Yao, C.L., Trial, F., and Parker, D.M. (1995). Role of cutinase in the invasion of plants. *Can. J. Bot.* **73** (suppl.): S1109–S1118.
- Kulkarni, R.D., Kelkar, H.S., and Dean, R.A. (2003). An eight-cysteine-containing CFEM domain unique to a group of fungal membrane proteins. *Trends Biochem. Sci.* **28**: 118–121.
- Kulkarni, R.D., Thon, M.R., Pan, H.Q., and Dean, R.A. (2005). Novel G-protein-coupled receptor-like proteins in the plant pathogenic fungus *Magnaporthe grisea*. *Genome Biol.* **6**: R24.
- Kurdyukov, S., Faust, A., Nawrath, C., Bar, S., Voisin, D., Efremova, N., Franke, R., Schreiber, L., Saedler, H., Metraux, J.P., and Yephremov, A. (2006). The epidermis-specific extracellular BODY-GUARD controls cuticle development and morphogenesis in *Arabidopsis*. *Plant Cell* **18**: 321–339.
- Lee, N., D'Souza, C.A., and Kronstad, J.W. (2003). Of smuts, blights, mildews, and blights: cAMP signaling in phytopathogenic fungi. *Annu. Rev. Phytopathol.* **41**: 399–427.
- Lee, Y.H., and Dean, R.A. (1993). cAMP regulates infection structure formation in the plant pathogenic fungus *Magnaporthe grisea*. *Plant Cell* **5**: 693–700.
- Lee, Y.H., and Dean, R.A. (1994). Hydrophobicity of contact surface induces appressorium formation in *Magnaporthe grisea*. *FEMS Microbiol. Lett.* **115**: 71–75.
- Lees, K., Roberts, S., Skamnioti, P., and Gurr, S.J. (2007). Gene microarray analysis using angular distribution decomposition. *J. Comput. Biol.* **14**: 68–83.
- Lequeu, J., Fauconnier, M.L., Chammai, A., Bronner, R., and Blee, E. (2003). Formation of plant cuticle: Evidence for the occurrence of the peroxygenase pathway. *Plant J.* **36**: 155–164.
- Li, D.H., Ashby, A.M., and Johnstone, K. (2003). Molecular evidence that the extracellular cutinase Pbc1 is required for pathogenicity of *Pyrenopeziza brassicae* on oilseed rape. *Mol. Plant Microbe Interact.* **16**: 545–552.
- Li, D.X., Sirakova, T., Rogers, L., Ettinger, W.F., and Kolattukudy, P.E. (2002). Regulation of constitutively expressed and induced cutinase genes by different zinc finger transcription factors in *Fusarium solani* f. sp. *pisi* (*Nectria haematococca*). *J. Biol. Chem.* **277**: 7905–7912.
- Liu, H., Suresh, A., Willard, F.S., Siderovski, D.P., Lu, S., and Naqvi, N.I. (2007). Rgs1 regulates multiple G alpha subunits in *Magnaporthe* pathogenesis, asexual growth and thigmotropism. *EMBO J.* **26**: 690–700.
- Liu, S.H., and Dean, R.A. (1997). G protein alpha subunit genes control growth, development, and pathogenicity of *Magnaporthe grisea*. *Mol. Plant Microbe Interact.* **10**: 1075–1086.
- Maiti, I.B., and Kolattukudy, P.E. (1979). Prevention of fungal infection of plants by specific inhibition of cutinase. *Science* **205**: 507–508.
- Marek, A., and Bednarski, W. (1996). Some factors affecting lipase production by yeasts and filamentous fungi. *Biotechnol. Lett.* **18**: 1155–1160.
- Martinez, C., Degeus, P., Lauwereys, M., Matthysens, G., and Cambillau, C. (1992). *Fusarium solani* cutinase is a lipolytic enzyme with a catalytic serine accessible to solvent. *Nature* **356**: 615–618.
- Mitchell, T.K., and Dean, R.A. (1995). The cAMP-dependent protein-kinase catalytic subunit is required for appressorium formation and pathogenesis by the rice blast pathogen *Magnaporthe grisea*. *Plant Cell* **7**: 1869–1878.
- Murphy, C.A., Cameron, J.A., Huang, S.J., and Vinopal, R.T. (1996). *Fusarium* polycaprolactone depolymerase is cutinase. *Appl. Environ. Microbiol.* **62**: 456–460.
- Murphy, S.C., Harrison, T., Hamm, H.E., Lomasney, J.W., Mohandas, N., and Haldar, K. (2006). Erythrocyte G protein as a novel target for malarial chemotherapy. *PLoS Med.* **3**: 2403–2415.
- Nawrath, C. (2006). Unraveling the complex network of cuticular structure and function. *Curr. Opin. Plant Biol.* **9**: 281–287.
- Nishimura, M., Park, G., and Xu, J.R. (2003). The G-beta subunit MGB1 is involved in regulating multiple steps of infection-related morphogenesis in *Magnaporthe grisea*. *Mol. Microbiol.* **50**: 231–243.
- O'Toole, G.A., Pratt, L.A., Watnick, P.I., Newman, D.K., Weaver, V.B., and Kolter, R. (1999). Genetic approaches to the study of biofilms. *Methods Enzymol.* **310**: 91–109.
- Park, G., Bruno, K.S., Staiger, C.J., Talbot, N.J., and Xu, J.R. (2004). Independent genetic mechanisms mediate turgor generation and penetration peg formation during plant infection in the rice blast fungus. *Mol. Microbiol.* **53**: 1695–1707.
- Park, G., Xue, G.Y., Zheng, L., Lam, S., and Xu, J.R. (2002). MST12 regulates infectious growth but not appressorium formation in the rice blast fungus *Magnaporthe grisea*. *Mol. Plant Microbe Interact.* **15**: 183–192.
- Pascholati, S.F., Deising, H., Leite, B., Anderson, D., and Nicholson, R.L. (1993). Cutinase and nonspecific esterase activities in the conidial mucilage of *Colletotrichum graminicola*. *Physiol. Mol. Plant Pathol.* **42**: 37–51.
- Pascholati, S.F., Yoshioka, H., Kunoh, H., and Nicholson, R.L. (1992). Preparation of the infection court by *Erysiphe graminis* f. sp. *hordei* - Cutinase is a component of the conidial exudate. *Physiol. Mol. Plant Pathol.* **41**: 53–59.
- Pfaffl, M.W. (2001). A new mathematical model for relative quantification in real-time RT-PCR. *Nucleic Acids Res.* **29**: e45.

- Podila, G.K., Dickman, M.B., and Kolattukudy, P.E.** (1988). Transcriptional activation of a cutinase gene in isolated fungal nuclei by plant cutin monomers. *Science* **242**: 922–925.
- Purdy, R.E., and Kolattukudy, P.E.** (1975). Hydrolysis of plant cuticle by plant pathogens - Purification, amino acid composition, and molecular weight of two isoenzymes of cutinase and a nonspecific esterase from *Fusarium solani* f.sp. *pisi*. *Biochemistry* **14**: 2824–2831.
- Reis, H., Pfiffi, S., and Hahn, M.** (2005). Molecular and functional characterization of a secreted lipase from *Botrytis cinerea*. *Mol. Plant Pathol.* **6**: 257–267.
- Rogers, L.M., Flaishman, M.A., and Kolattukudy, P.E.** (1994). Cutinase gene disruption in *Fusarium solani* f.sp. *pisi* decreases its virulence on pea. *Plant Cell* **6**: 935–945.
- Sambrook, J., and Russell, D.W.** (2001). *Molecular Cloning: A Laboratory Manual*. (Cold Spring Harbor, NY: Cold Spring Harbor Laboratory Press).
- Schweizer, P., Jeanguenat, A., Mossinger, E., and Metraux, J.P.** (1994). Plant protection by free cutin monomers in two cereal pathosystems. In *Advances in Molecular Genetics of Plant-Microbe Interactions*, M.J. Daniels, J.A. Downie, and A.E. Osbourn, eds (Dordrecht, The Netherlands: Kluwer Academic Publishers), pp. 371–374.
- Schweizer, P., Jeanguenat, A., Whitacre, D., Metraux, J.P., and Mosinger, E.** (1996). Induction of resistance in barley against *Erysiphe graminis* f.sp. *hordei* by free cutin monomers. *Physiol. Mol. Plant Pathol.* **49**: 103–120.
- Sieber, P., Schorderet, M., Ryser, U., Buchala, A., Kolattukudy, P., Metraux, J.P., and Nawrath, C.** (2000). Transgenic *Arabidopsis* plants expressing a fungal cutinase show alterations in the structure and properties of the cuticle and postgenital organ fusions. *Plant Cell* **12**: 721–737.
- Skamnioti, P., Henderson, C., Zhang, Z., Robinson, Z., and Gurr, S.J.** (2007). A novel role for catalase B in the maintenance of fungal cell wall integrity during host invasion in the rice blast fungus *Magnaporthe grisea*. *Mol. Plant Microbe Interact.* **20**: 568–580.
- Stahl, D.J., and Schafer, W.** (1992). Cutinase is not required for fungal pathogenicity on pea. *Plant Cell* **4**: 621–629.
- Stahl, D.J., Theuerkauf, A., Heitefuss, R., and Schafer, W.** (1994). Cutinase of *Nectria haematococca* (*Fusarium solani* f.sp. *pisi*) is not required for fungal virulence or organ specificity on pea. *Mol. Plant Microbe Interact.* **7**: 713–725.
- Sweigard, J.A., Chumley, F.G., and Valent, B.** (1992a). Disruption of a *Magnaporthe grisea* cutinase gene. *Mol. Gen. Genet.* **232**: 183–190.
- Sweigard, J.A., Chumley, F.G., and Valent, B.** (1992b). Cloning and analysis of *Cut1*, a cutinase gene from *Magnaporthe grisea*. *Mol. Gen. Genet.* **232**: 174–182.
- Talbot, N.J.** (2003). On the trail of a cereal killer: Exploring the biology of *Magnaporthe grisea*. *Annu. Rev. Microbiol.* **57**: 177–202.
- Talbot, N.J., Ebbole, D.J., and Hamer, J.E.** (1993). Identification and characterization of *Mpg1*, a gene involved in pathogenicity from the rice blast fungus *Magnaporthe grisea*. *Plant Cell* **5**: 1575–1590.
- Talbot, N.J., Kershaw, M.J., Wakley, G.E., deVries, O.M.H., Wessels, J.G.H., and Hamer, J.E.** (1996). *MPG1* encodes a fungal hydrophobin involved in surface interactions during infection-related development of *Magnaporthe grisea*. *Plant Cell* **8**: 985–999.
- Thines, E., Eilbert, F., Sterner, O., and Anke, H.** (1997a). Glisoprenin A, an inhibitor of the signal transduction pathway leading to appressorium formation in germinating conidia of *Magnaporthe grisea* on hydrophobic surfaces. *FEMS Microbiol. Lett.* **151**: 219–224.
- Thines, E., Eilbert, F., Sterner, O., and Anke, H.** (1997b). Signal transduction leading to appressorium formation in germinating conidia of *Magnaporthe grisea*: Effects of second messengers diacylglycerols, ceramides and sphingomyelin. *FEMS Microbiol. Lett.* **156**: 91–94.
- Tucker, S.L., and Talbot, N.J.** (2001). Surface attachment and pre-penetration stage development by plant pathogenic fungi. *Annu. Rev. Phytopathol.* **39**: 385–417.
- Valent, B.** (1990). Rice blast as a model system for plant pathology. *Phytopathology* **80**: 33–36.
- Valent, B., Farrall, L., and Chumley, F.G.** (1991). *Magnaporthe grisea* genes for pathogenicity and virulence identified through a series of backcrosses. *Genetics* **127**: 87–101.
- van Kan, J.A.L., van't Klooster, J.W., Wagemakers, C.A., Dees, D.C., and van der Vlugt-Bergmans, C.J.** (1997). Cutinase A of *Botrytis cinerea* is expressed, but not essential, during penetration of gerbera and tomato. *Mol. Plant Microbe Interact.* **10**: 30–38.
- Wang, Z.Y., Jenkinson, J.M., Holcombe, L.J., Soanes, D.M., Veneault-Fourrey, C., Bhambra, G.K., and Talbot, N.J.** (2005). The molecular biology of appressorium turgor generation by the rice blast fungus *Magnaporthe grisea*. *Biochem. Soc. Trans.* **33**: 384–388.
- Woloshuk, C.P., and Kolattukudy, P.E.** (1986). Mechanism by which contact with plant cuticle triggers cutinase gene expression in the spores of *Fusarium solani* f.sp. *pisi*. *Proc. Natl. Acad. Sci. USA* **83**: 1704–1708.
- Xu, J.R., and Hamer, J.E.** (1996). MAP kinase and cAMP signaling regulate infection structure formation and pathogenic growth in the rice blast fungus *Magnaporthe grisea*. *Genes Dev.* **10**: 2696–2706.
- Xu, J.R., Staiger, C.J., and Hamer, J.E.** (1998). Inactivation of the mitogen-activated protein kinase *Mps1* from the rice blast fungus prevents penetration of host cells but allows activation of plant defense responses. *Proc. Natl. Acad. Sci. USA* **95**: 12713–12718.
- Xu, J.R., Urban, M., Sweigard, J.A., and Hamer, J.E.** (1997). The *cPKA* gene of *Magnaporthe grisea* is essential for appressorial penetration. *Mol. Plant Microbe Interact.* **10**: 187–194.
- Yao, C.L., and Koller, W.** (1995). Diversity of cutinases from plant-pathogenic fungi - Different cutinases are expressed during saprophytic and pathogenic stages of *Alternaria brassicicola*. *Mol. Plant Microbe Interact.* **8**: 122–130.
- Zhang, Z., Henderson, C., Perfect, E., Carver, T.L.W., Thomas, B.J., Skamnioti, P., and Gurr, S.J.** (2005). Of genes and genomes, needles and haystacks: *Blumeria graminis* and functionality. *Mol. Plant Pathol.* **6**: 561–575.
- Zhang, Z., Priddey, G., and Gurr, S.J.** (2001). The *Erysiphe graminis* protein kinase C gene *pkc1* and *pkc*-like gene are differentially regulated during germling morphogenesis. *Mol. Plant Pathol.* **2**: 327–338.
- Zhao, X.H., Kim, Y., Park, G., and Xu, J.R.** (2005). A mitogen-activated protein kinase cascade regulating infection-related morphogenesis in *Magnaporthe grisea*. *Plant Cell* **17**: 1317–1329.